JCI insight

Epithelial microRNA-206 targets CD39/extracellular ATP to upregulate airway IL-25 and TSLP in type 2-high asthma

Kan Zhang, … , Dan Cheng, Guohua Zhen

JCI Insight. 2021. https://doi.org/10.1172/jci.insight.148103.

Research In-Press Preview Pulmonology

Graphical abstract

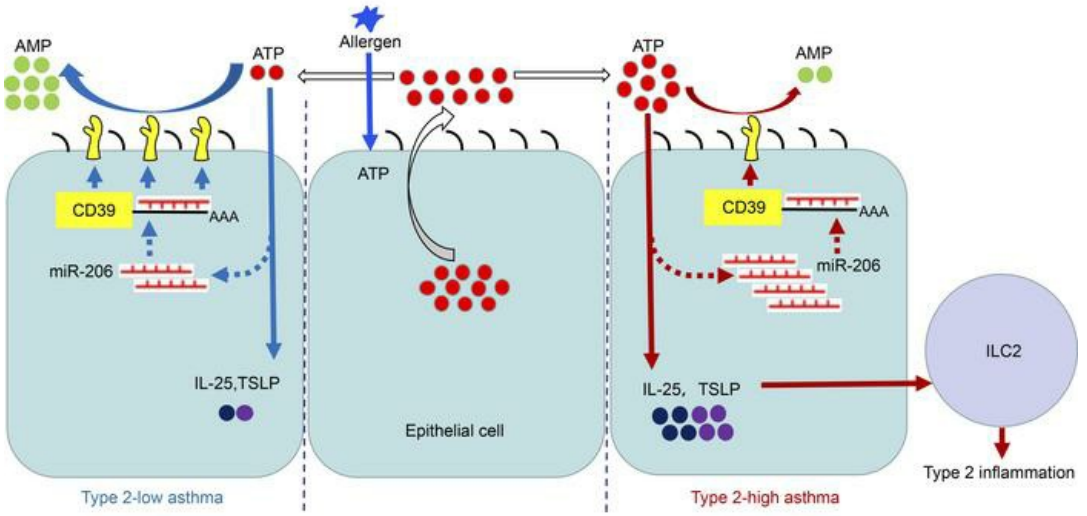

Epithelial microRNA-206 targets CD39/extracellular ATP to upregulate airway IL-25 and TSLP in type 2-high asthma

Kan Zhang[1,2,3]*, Yuchen Feng[1,2]*, Yuxia Liang[1,2], Wenliang Wu[1,2], Chenli Chang[1,2], Dian Chen[1,2], Shengchong Chen[1,2], Jiali Gao[1,2], Gongqi Chen[1,2], Lingling Yi[1,2], Dan Cheng[4], Guohua Zhen[1,2]†

[1]Division of Pulmonary and Critical Care Medicine, Department of Internal Medicine, Tongji Hospital, Tongji Medical College, Huazhong University of Science and Technology, Wuhan, China; [2]Key Laboratory of Respiratory Diseases, National Health Commission of People's Republic of China, and National Clinical Research Center for Respiratory Diseases, Wuhan, China; [3]Department of Respiratory and Critical Care Medicine, The Affiliated Suzhou Hospital of Nanjing Medical University, Suzhou, China; [4]Department of Respiratory and Critical Care Medicine, Renmin Hospital of Wuhan University, Wuhan, China.

***** KZ and YF contributed equally to this work.

†Correspondence to: Guohua Zhen, Division of Respiratory and Critical Care Medicine, Tongji Hospital, Wuhan, China 430030; Email: ghzhen@tjh.tjmu.edu.cn

Conflict of interest: The authors have declared that no conflict of interest exists.

Short title: MicroRNA 206 upregulates IL-25 and TSLP in asthma

ABSTRACT:

The epithelial cell-derived cytokines IL-25, IL-33 and TSLP initiate type 2 inflammation in allergic diseases including asthma. However, the signaling pathway regulating these cytokines expression remains elusive. Since microRNAs are pivotal regulators of gene expression, we profiled microRNA expression in bronchial epithelial brushings from type 2-low and type 2-high asthma patients. MiR-206 was the most highly expressed epithelial microRNA in type 2-high asthma relative to type 2-low asthma but was downregulated in both subsets compared with healthy controls. CD39, an ectonucleotidase degrading ATP, was a target of miR-206 and upregulated in asthma. Allergen-induced acute extracellular ATP accumulation led to miR-206 downregulation and CD39 upregulation in human bronchial epithelial cells, forming a feedback loop to eliminate excessive ATP. Airway ATP levels were markedly elevated and strongly correlated with IL-25 and TSLP expression in asthma patients. Intriguingly, airway miR-206 antagonism increased Cd39 expression, reduced ATP accumulation, suppressed Il-25, Il-33, Tslp expression and group 2 innate lymphoid cell expansion, and alleviated type 2 inflammation in a mouse model of allergic airway inflammation. In contrast, airway miR-206 overexpression had opposite effects. Overall, epithelial miR-206 upregulates airway IL-25, TSLP expression by targeting CD39-extracellular ATP axis, which represents a novel therapeutic target in type 2-high asthma.

Keywords: asthma; epithelial cells; microRNA; CD39; extracellular ATP; IL-25; TSLP

INTRODUCTION

Asthma is a heterogeneous disease with different phenotypes, endotypes, and variable responses to management approaches (1, 2). A prominent endotype of asthma is the presence of type 2 inflammation (3, 4). Airway epithelial cells play pivotal roles in the initiation of type 2 inflammation by expressing interleukin (IL)-25, IL-33 and thymic stromal lymphopoietin (TSLP) (5-7). These epithelial cell-derived cytokines act on innate immune cells including dendritic cells, group 2 innate lymphoid cells (ILC2s) and mast cells (8-15). Recent identification of memory Th2 cells with high expression of receptors for IL-25, IL-33 and TSLP supports a role of these cytokines in adaptive immune responses in allergy (16, 17). IL-25 (18, 19), IL-33 (20), and TSLP (11) have each been reported to be indispensable and sufficient for type 2 cytokine production, eosinophilic airway inflammation and AHR in certain mouse models. In human asthma, various expression patterns of these cytokines have been reported (21-25). Although IL-25, IL-33 and TSLP are critical in type 2 airway inflammation, the upstream signaling pathway regulating their expression remains elusive.

When exposed to environmental stimuli, airway epithelial cells rapidly express danger signals such as adenosine triphosphate (ATP) and uric acid to alert the immune system (26, 27). Allergen exposure enhanced airway ATP concentrations in human asthma and sensitized mice. Neutralizing airway ATP or blocking purine signaling suppressed airway inflammation in allergen-sensitized and challenged mice (28). The extracellular ATP concentration is tightly controlled by ecto-nucleoside triphosphate diphosphohydrolases (ENTPDs) (29). CD39 (encoded by *ENTPD1*) catalyzes the degradation of extracellular ATP and ADP and is expressed in airway epithelial cells (30). Inhibition of Cd39 activity increased the BALF ATP concentration and intensified

ovalbumin-induced bronchospasm in mice (31). *Cd39*-deficient mice exhibited worsened airway inflammation and mucus overproduction after allergen sensitization and challenge (32), whereas paradoxically alleviated airway inflammation was also reported in *Cd39*-deficient mice (33). Recently, it was reported that ATP serves as a sensor for an airborne allergen to trigger IL-33 release in airway epithelial cells (34). Together, these studies suggest that the CD39-extracellular ATP axis may regulate IL-25, IL-33 and TSLP in asthma.

MicroRNAs (miRNAs) regulate gene expression by promoting the catabolism of the target transcripts as well as attenuating their translation. A growing body of evidence indicates that miRNAs play important roles in epithelial cell, ILC2 and Th2 cell differentiation and function in asthma (35-38). MiR-19a promotes IL-5 and IL-13 expression in ILC2s and Th2 cells (37, 38). Let-7 miRNA regulates IL-13 expression and allergic airway inflammation (39, 40). Global miRNA expression in airway epithelial cells is altered in asthma (36, 41). However, the difference in epithelial miRNA expression between type 2-low and type 2-high asthma remains unknown. We hypothesized that the differentially expressed epithelial miRNAs between the two asthma subsets may contribute to IL-25, IL-33 and TSLP expression in asthma.

In this study, we profiled the epithelial miRNA expression in type 2-low and type 2-high asthma patients. We found that miR-206, the most highly expressed miRNA in type 2-high asthma relative to type 2-low asthma, targets the CD39-extracelluar ATP axis to regulate IL-25 and TSLP expression in cultured bronchial epithelial cells. Airway ATP levels were increased and strongly correlated with elevated IL-25 and TSLP expression in type 2-high asthma patients. In a mouse model of asthma, manipulation of airway miR-206 expression altered Il-25, Il-33, and Tslp expression, ILC2 expansion, and type 2 airway inflammation.

RESULTS

Differentially expressed epithelial miRNAs, including miR-206, between type 2-low and type 2–high asthma.

We profiled miRNA expression in bronchial epithelial brushings from type 2-low asthmatics (*n* = 4) and type 2-high asthmatics (*n* = 4) using a miRNA microarray. The type 2 status of asthma was defined by the expression of the type 2 signature genes (*CLCA1*, *POSTN*, and *SERPINB10*) in the epithelial brushings as previously reported (3, 42). We found that 20 miRNAs were significantly differentially expressed between the two subsets of asthma (Figure 1A). The data are available at GEO (http://www.ncbi.nlm.nih.gov/geo/, accession number GSE142237). Of note, miR-206 was the most highly expressed miRNA in type 2-high asthma relative to type 2-low asthma. Several other differentially expressed miRNAs including miR-31-5p, miR-146a-5p, miR-146b-5p, and miR-221-3p have been implicated in asthma pathogenesis (43-45). Epithelial miR-221-3p expression was shown to be associated with airway eosinophilia and the expression of type 2 signature genes in asthma patients in our previous study (46).

We next examined the expression of miR-206 in a cohort including type 2-low asthmatics (*n* = 20), type 2-high asthmatics (*n* = 37), and healthy controls (*n* = 26) using quantitative PCR. Compared with type 2-low asthmatics, type 2-high asthmatics had lower methacholine PD_{20}, higher eosinophil counts in induced sputum and blood, and higher fractional exhaled nitric oxide (FeNO) and serum IgE levels (Table 1). Consistent with the microarray data, epithelial miR-206 expression was higher in type 2-high asthma than in type 2-low asthma. However, compared to healthy controls, epithelial miR-206 transcript levels were decreased in both type 2-low and type 2-high asthma (Figure 1B). Our data suggest that epithelial miR-206 expression is downregulated

in asthma and associates with airway type 2 inflammation.

The expression of CD39, a target of miR-206, is upregulated in airway epithelial cells in asthma

We predicted candidate target genes of miR-206 by using online algorithms (DIANA-microT, miRanda, miRWalk, PicTar and TargetScan). CD39 (encoded by *ENTPD1*), the ectoenzyme catalyzing the degradation of extracellular ATP and ADP, was one of the candidate targets. The 3'-untranslated region (UTR) of *CD39* contains nucleotides matching the seed sequence of *hsa-miR-206* (Figure 1C). Transfection with the miR-206 mimic decreased the luciferase activity when co-transfected with the vector harboring the wild-type *CD39* 3'-UTR, but had no effect on the luciferase activity when co-transfected with the vector containing the mutant 3'-UTR or empty vector (Figure 1D). This indicates that miR-206 may directly act on the 3'-UTR of *CD39* mRNA. Furthermore, inhibition of miR-206 expression enhanced CD39 mRNA and protein expression, whereas overexpression of miR-206 suppressed CD39 expression (Figure 1E-G). These data indicate that *CD39* is a target of miR-206.

In human asthma, we found that *CD39* transcript levels were significantly increased in bronchial brushings from type 2-low and -high asthma patients compared to controls. Moreover, epithelial *CD39* expression was lower in type 2-high asthma than in type 2-low asthma (Figure 1H). In support of *CD39* as a target of miR-206, epithelial *CD39* transcript levels negatively correlated with epithelial miR-206 expression in asthma patients (Figure 1I).

Extracellular ATP accumulation induces miR-206 downregulation and CD39 upregulation in human bronchial epithelial cells

It was reported that BALF ATP concentration was increased in asthma patients after allergen

provocation (28). In BALF from our symptomatic and treatment-naïve asthma patients, we measured ATP using luciferase bioluminescence. BALF ATP levels were markedly increased in both type 2-low and type 2–high asthma patients compared to controls (Figure 2A). Moreover, BALF ATP levels were higher in type 2-high asthma than in type 2-low asthma. This suggests that extracellular ATP accumulates in the airways of symptomatic asthma patients.

Extracellular ATP accumulation upregulates CD39 expression in airway epithelial cells, which catalyzes degradation of excessive extracellular ATP to maintain the homeostasis in the microenvironment (47). To determine whether the miR-206-CD39 axis responds to extracellular ATP accumulation, we performed air-liquid interface culture of human bronchial epithelial (HBE) cells from healthy donors. House dust mite (HDM), the most clinically relevant allergen, rapidly increased ATP concentrations in culture medium within 2 min. The ATP concentration peaked at 1-2 h, and declined to baseline by 6 h (Figure 2B). HDM exposure decreased miR-206 expression from 2 h to 12 h, with maximum inhibition at 6 h (Figure 2C), and increased the *CD39* mRNA level from 2 h to 12 h, peaking at 6 h (Figure 2D). Furthermore, elimination of extracellular ATP by pretreatment with apyrase suppressed HDM-induced miR-206 downregulation and CD39 upregulation at 6 h in HBE cells (Figure 2E and G). The exogenous ATP analog ATPγS directly decreased miR-206 expression, increased CD39 expression and intensified HDM-induced miR-206 downregulation and CD39 upregulation (Figure 2F and H). Similarly, we found that Alternaria-induced extracellular ATP accumulation was also required for miR-206 downregulation and CD39 upregulation in BEAS-2B cells (Supplementary Figure 1). Together, our data suggest that allergen-induced acute accumulation of extracellular ATP downregulates miR-206 and upregulates CD39 expression in airway epithelial cells. This may represent a protective

mechanism to eliminate excessive extracellular ATP.

Higher ATP levels are associated with elevated IL-25 and TSLP expression in type 2-high asthma

Allergens stimulate the release of ATP as an alarmin from airway epithelial cells to induce the expression of IL-33 (34). We next examined airway IL-25, IL-33 and TSLP expression in bronchial epithelial brushings and BALF using quantitative PCR and ELISA, respectively. Epithelial *IL25* transcript levels and BALF IL-25 protein levels were significantly higher in type 2-high asthma patients than in type 2-low asthma patients and controls (Figure 3A, 3D). There were multiple splice variants of the *IL33* transcript, and the protein encoded by the *IL33* transcript without exons 3 and 4 was secreted as an active cytokine (48). We examined the expression of *IL33* transcripts without exons 3 and 4 in bronchial epithelial brushings using RNase H-dependent quantitative PCR as previously reported (48). However, there were no significant differences in this *IL33* transcript between the two asthma subsets and controls. Additionally, we did not detect a significant difference in IL-33 protein levels in BALF (Figure 3B, 3E). TSLP has short and long isoforms, and the long isoform is induced during inflammation (49). We found that the long *TSLP* transcripts and BALF TSLP protein levels were higher in type 2-high asthma patients than in type 2-low asthma patients and control subjects (Figure 3C, 3F). Our data suggest that airway expression of IL-25 and TSLP, but not IL-33, is elevated in type 2-high asthma.

Importantly, BALF ATP levels were strongly correlated with BALF IL-25 and TSLP protein levels (Figure 3G-H). This indicates that the more prominent accumulation of airway ATP may be responsible for the elevated IL-25 and TSLP expression in type 2-high asthma.

Extracellular ATP is essential for allergen-induced IL-25 and TSLP expression in human

bronchial epithelial cells.

We next examined the role of extracellular ATP in HDM-induced IL-25, IL-33 and TSLP expression in HBE cells cultured on an air-liquid interface. We found that HDM stimulation increased *IL25* mRNA expression in HBE cells and IL-25 protein levels in basal-lateral medium, peaking at 2 h and 6 h, respectively (Figure 4A and D). HDM also increased *TSLP* (the long transcript variant) mRNA and protein expression, which peaked at 1 h and 6 h, respectively (Figure 4C and F). However, HDM stimulation did not alter the expression of *IL33* (the transcript without exons 3 and 4) mRNA or protein (Figure 4B and E). Elimination of extracellular ATP through CD39 overexpression or by using apyrase suppressed HDM-induced IL-25 and TSLP protein expression at 6 h (Figure 4G-J). In contrast, enhancing extracellular ATP by CD39 knockdown or by adding ATPγS further increased HDM-induced IL-25 and TSLP protein expression (Figure 4K-N). Similarly, Alternaria-induced extracellular ATP accumulation promoted IL-25 and TSLP expression in BEAS-2B cells (Supplementary Figure 2). These data suggest that allergen-induced acute extracellular ATP accumulation is required for IL-25 and TSLP upregulation in airway epithelial cells.

MiR-206 regulates allergen-induced IL-25 and TSLP expression in bronchial epithelial cells via targeting the CD39-extracellular ATP axis

We next examined whether miR-206 regulates IL-25 and TSLP expression via targeting the CD39-extracellular ATP axis in HDM-stimulated HBE cells. Inhibition of miR-206 expression by transfection with miR-206 inhibitor increased baseline and HDM-induced CD39 expression. Importantly, inhibition of miR-206 expression decreased the ATP concentration and suppressed HDM-induced IL-25 and TSLP protein expression in the medium (Supplementary Figure 3A-D).

In contrast, miR-206 overexpression by transfection with miR-206 mimic suppressed baseline and HDM-induced CD39 expression, enhanced extracellular ATP, and further enhanced HDM-induced IL-25 and TSLP protein expression (Supplementary Figure 1E-H). Our data indicate that miR-206 regulates epithelial IL-25 and TSLP expression by targeting the CD39-extracellular ATP axis.

Airway epithelial miR-206 regulates CD39 expression and BALF ATP concentration in a murine model of allergic airway disease

We investigated the role of epithelial miR-206 in a murine model of allergic airway inflammation. C57BL/6 mice were sensitized and challenged with HDM (Figure 5A). The 3'-UTR of the mouse *Cd39* gene has binding sites for the seed region of *mmu-miR-206-3p* which is identical to *hsa-miR-206* (Figure 5B). Using quantitative PCR, in situ hybridization, immunohistochemistry and luciferase bioluminescence, we found that HDM challenge decreased epithelial miR-206 expression, increased Cd39 expression, and markedly enhanced BALF ATP levels compared to control mice. Inhibition of airway miR-206 expression by intranasal administration of miR-206 antagomir further enhanced HDM-induced Cd39 expression but suppressed HDM-induced BALF ATP accumulation (Figure 5C-E). In contrast, airway overexpression of miR-206 induced by intranasal administration of miR-206 agomir significantly suppressed HDM-induced Cd39 expression and further enhanced the HDM-induced increase in ATP concentrations (Figure 5F-J). These data suggest that epithelial miR-206 targets the Cd39-extracellular ATP axis in the airway of a murine model of allergic airway disease.

Airway miR-206 antagonism suppresses HDM-induced AHR, airway eosinophilia, mucus overproduction and type 2 cytokines expression in mice

In the murine model of allergic airway disease, HDM sensitization and challenge increased

airway resistance to methacholine, induced infiltration of inflammatory cells around airways, and increased airway mucus-producing cells, *Muc5ac* expression, and plasma IgE levels. Inhibition of airway miR-206 expression by transfection with miR-206 antagomir significantly suppressed HDM-induced AHR, airway eosinophilic inflammation and mucus overproduction (Figure 6A-G). In contrast, airway miR-206 overexpression induced by transfection with miR-206 agomir further enhanced HDM-induced AHR, airway eosinophilia and mucus overproduction (Supplementary Figure 4A-G). Moreover, airway miR-206 antagonism suppressed HDM-induced expression of type 2 cytokines including Il-4, Il-5 and Il-13, and decreased plasma IgE levels (Figure 6H-K), whereas miR-206 overexpression further enhanced HDM-induced expression of type 2 cytokines in mouse lungs and plasma IgE levels (Supplementary Figure 4H-K). Our data indicate that epithelial miR-206 plays an essential role in allergic airway disease by regulating the type 2 immune response.

Airway miR-206 antagonism suppresses Il-25, Il-33, and Tslp expression and ILC2 expansion in mice

Since ILC2s play a pivotal role in the type 2 response upon activation by IL-25, IL-33 and TSLP, we further examined the effect of airway miR-206 manipulation on Il-25, Il-33, and Tslp expression and ILC2 expansion in mice. HDM sensitization and challenge increased Il-25, Il-33 and Tslp protein levels in BALF (Figure 7A-F). Meanwhile, flow cytometric analysis revealed that HDM sensitization and challenge significantly increased the number of ILC2s ($Lin^-CD25^+CD127^+ST2^+Sca\text{-}1^+$ cells, gating strategy in Figure 7G) in single-cell suspensions of lungs (Figure 7H-K). Airway miR-206 antagonism suppressed HDM-induced Il-25, Il-33, and Tslp expression (Figure 7A-C) and ILC2 expansion (Figure 7H and J), whereas miR-206

overexpression further enhanced HDM-induced Il-25, Il-33 and Tslp expression (Figure 7D-F) and ILC2 expansion in mouse lungs (Figure 7I and K). This suggests that epithelial miR-206 regulates HDM-induced Il-25, Il-33 and Tslp expression and ILC2 expansion in mouse models.

DISCUSSION

In the present study, we reported that epithelial miR-206 was differentially expressed between type 2-low and -high asthma patients who were symptomatic and treatment-naïve. Type 2-high asthma patients had higher miR-206 expression, lower epithelial CD39 expression, elevated BALF ATP levels, and higher epithelial IL-25 and TSLP expression than type 2-low asthma patients. Of note, BALF ATP levels were strongly correlated with airway IL-25 and TSLP expression in asthma patients. The associations between these measurements were functionally validated in primary cultured of HBE cells and in a murine model of allergic airway inflammation.

MiRNAs play essential roles in the pathogenesis of asthma (39, 40, 50, 51). To date, the differentially expressed epithelial miRNAs between type 2-low and type 2-high asthma remain unknown. We identified miR-206 as the most highly expressed miRNA in type 2-high asthma relative to type 2-low asthma. However, compared to control subjects, miR-206 expression was downregulated in both asthma subsets. MiR-206 expression was also decreased in cultured HBE cells exposed to HDM and in the airways of mice sensitized and challenged with HDM. Our findings are consistent with a study reporting that miR-206 expression was decreased in the airway wall of a mouse model of childhood allergic asthma (52). Recent studies have showed that miR-206 expression is also decreased in mouse models of occupational asthma (53, 54). In humans, it was reported that circulating miR-206 was useful to predict childhood asthma exacerbation (55), and plasma miR-206 expression differed between asthmatics with higher and lower blood eosinophil counts (56). However, the mechanism underlying the less reduction in epithelial miR-206 in type 2-high asthma than in type 2-low asthma requires further investigation. It was reported that production of reactive oxygen species (ROS) upregulated miR-206 expression

(57, 58). Interestingly, IL-13, a type 2 cytokine, promotes ROS production in airway epithelial cells (59). Thus, one possibility for higher miR-206 expression in type 2-high asthma is that type 2 cytokine-induced ROS production upregulated miR-206 expression.

To explore the role of miR-206 in asthma, we verified that CD39, an ecto-nucleotidase that degrades ATP, was a target of miR-206. To date, there are no studies addressing the regulation of airway CD39 in human asthma. Previous reports regarding the role of Cd39 in animal asthma models are conflicting (32, 33). We demonstrated that CD39 expression was increased in the airway epithelium in human asthma and in mice sensitized and challenged with HDM. Consistent with the higher expression of miR-206 in type 2-high asthma, CD39 expression was lower in type 2-high asthma than in type 2-low asthma.

Extracellular ATP serves as a danger signal to alert the immune system of damaged tissue. In our cohort of symptomatic and treatment-naïve asthma patients, BALF ATP concentrations were significantly increased, especially in type 2-high asthma patients. This is consistent with a previous report that allergen provocation enhanced airway BALF ATP accumulation in asthma patients (28). The elevated airway ATP levels in our asthma patients might be due to exposure to environmental aeroallergens, including HDM and/or airway virus infections, the main triggers of asthma exacerbation (12, 60). Rhinovirus infection has been reported to stimulate bronchial smooth muscle cells to release ATP (61), and influenza A virus infection was found to increase BALF ATP levels in mice (62).

In our in vitro system, we demonstrated that allergen-induced acute extracellular ATP accumulation was responsible for miR-206 downregulation and CD39 upregulation in HBE cells at an air-liquid interface. Since CD39 catalyzes ATP degradation, the CD39 upregulation in

asthma patients and in allergen-exposed epithelial cells may represent an inhibitory feedback response to excessive ATP, by which striving to maintain airway homeostasis.

In human asthma, we previously reported that epithelial *IL25* mRNA expression was upregulated in a subset of asthma patients featured by type 2 inflammation (63). Here, in a different cohort of asthmatic patients, using ELISA and qPCR, we found that airway expression of IL-25 and TSLP, but not IL-33, was elevated in type 2-high asthma patients. The TaqMan qPCR primers and probes for the *IL33* isoform without exons 3 and 4, and the long isoform of *TSLP* were previously reported, and these isoforms were associated with type 2 inflammation (48, 49). To date, there have been few head-to-head studies of IL-25, IL-33 and TSLP expression in human asthma. Various expression patterns of these cytokines have been reported in different populations. In Korea, plasma IL-25, but not IL-33 or TSLP, was increased in patients with aspirin-exacerbated respiratory disease characterized by asthma, nasal polyps and chronic eosinophilic sinusitis (21). Elevated IL-25, but not IL-33 or TSLP mRNA, was reported in sputum cells from uncontrolled asthmatics in Belgium (22). In contrast, increased expression of IL-33 and TSLP, but not IL-25, was reported in asthma patients in London (23), Poland (24), and New York (25). This suggests that ethnicity and region should be considered in studies on these cytokines. Recently, a new concept “regiotype”, was introduced for allergic diseases, referring to regional differences between endotypes due to different allergens and other environmental influences (2). In chronic rhinosinusitis with nasal polyps (CRSwNP), a disease related to asthma, various expression patterns of IL-25, IL-33 and TSLP in different populations and regions have been described. Reports of IL-25 upregulation in CRSwNP have come from Asian countries including Korea (64), Japan (65) and China (66), whereas negative results for IL-25 were reported from the USA (67),

313 Australia (68) and Turkey (69). Our data on airway IL-25, IL-33 and TSLP expression in asthma
314 patients provide evidence for the novel therapies targeting these cytokines in China.

315 The upstream signaling pathway regulating the expression of epithelial IL-25 and TSLP remains
316 largely unknown. Extracellular ATP-activated purinergic receptors mediate aeroallergen-induced
317 IL-33 release from epithelial cells (34). Here we reported that BALF ATP concentrations were
318 strongly correlated with airway IL-25 and TSLP expression. In vitro, allergen-induced acute
319 accumulation of extracellular ATP was required and sufficient for IL-25 and TSLP expression.
320 Furthermore, epithelial miR-206 regulated IL-25 and TSLP expression by targeting the
321 CD39-extracellular ATP axis both in vitro and in vivo. HDM sensitization and challenge decreased
322 airway miR-206 expression while increasing Cd39 expression; BALF ATP concentration; Il-25,
323 Il-33 and Tslp expression; and ILC2 expansion in mice. Airway miR-206 antagonism before HDM
324 challenge suppressed Il-25, Il-33, and Tslp expression; ILC2 expansion; type 2 cytokine
325 expression; and the cardinal features of asthma in mice. On the other hand, miR-206
326 overexpression had the opposite effects. The explanation of the effect of miR-206 agomir
327 transfection should be cautious because non-specific effect of miRNA overexpression was
328 reported (70). In addition, intranasal administration of miR-206 agomir or antagomir may also
329 affect Cd39 expression in other cell types including macrophages in mice lungs.

330 As summarized in Figure 8, our findings suggest that epithelial miR-206 is downregulated in
331 both asthma subsets. Compared with type 2-low asthma, higher miR-206 expression resulted in
332 lower CD39 expression and impaired capacity to eliminate extracellular ATP in type 2-high
333 asthma. Consequently, more extracellular ATP was accumulated, leading to higher expression of
334 IL-25 and TSLP and more prominent type 2 inflammation in type 2-high asthma. The mechanism

underlying the impaired ability to downregulate miR-206 in response to excessive ATP in type 2-high asthma requires further study.

In conclusion, epithelial miR-206 regulates airway IL-25 and TSLP expression and type 2 inflammation in asthma by targeting the CD39-extracellular ATP axis. This pathway contributes, at least in part, to the development of human type 2-high asthma and represents a novel therapeutic target for this endotype.

METHODS

Human subjects

We recruited 26 healthy control subjects and 57 asthma patients who were symptomatic, newly diagnosed and treatment-naïve. All subjects were Chinese and were recruited from Tongji Hospital. Subjects with asthma were diagnosed by a physician; had symptoms of episodic cough, wheeze and/or dyspnea; and had an accumulated dosage of methacholine provoking a 20% fall (PD_{20}) in forced expiratory volume in the first second (FEV_1) < 2.505 mg and/or ≥12% increase in FEV_1 following inhalation of 200 μg salbutamol. We recruited subjects who had never smoked or received inhaled or oral corticosteroids or leukotriene antagonists. Healthy control subjects had no respiratory symptoms, normal spirometric values and a methacholine $PD_{20} \geq 2.505$ mg.

We recorded demographic information, performed spirometry, measured fractional exhaled nitric oxide (FeNO), and collected induced sputum. We performed bronchoscopy with bronchoalveolar lavage (BAL) and bronchial brushing. After inspection of the bronchial tree, 40 mL of prewarmed 0.9% saline was instilled into the right middle lobe and then gently aspirated. We brushed 10 sites within the subsegmental bronchi of the right middle and lower lobes (10 gentle upward and downward strokes per site). The dissociated cells were recovered in ice-cold DMEM.

MicroRNA microarray

Total RNA from bronchial epithelial brushing samples from four type 2-low and four type 2-high asthma patients was extracted using TRIzol (Invitrogen). After RNA quantity measurement using a NanoDrop 1000 spectrophotometer, the samples were labeled using a miRCURY Hy3/Hy5 power labeling kit (Exiqon) and hybridized on a miRCURY LNA microRNA array (7th generation,

miRBase v18; Exiqon). The slides were scanned using an Axon GenePix 4000B microarray scanner (Axon Instruments). Scanned images were then imported into GenePix Pro 6.0 software (Axon Instruments) for grid alignment and data extraction. We used the median normalization method to obtain "normalized data". Normalized data = (foreground - background) / median. In comparison, genes with greater than 2-fold change and that showed a statistically significant difference between the two groups were considered to be differentially expressed. The data are deposited at GEO (http://www.ncbi.nlm.nih.gov/geo/, accession number GSE142237).

Cell culture and treatment

Human bronchial epithelial (HBE) cells collected from heathy donors (n = 8) using the bronchial brushing technique were cultured on an air-liquid interface as previously described (71, 72). Briefly, ten sites of the subsegmental bronchi of the right middle and lower lobes were brushed. The dissociated cells were recovered by vortexing the brush in ice-cold DMEM. The cells were centrifuged, resuspended, seeded into six-well plates coated with collagen I from rat tails (Corning) and grown in bronchial epithelial cell medium (BEpiCM; ScienCell) with supplements. The medium was changed every 48 h until the cells were 90% confluent. Cells were then seeded on 1.1 cm^2 Transwell inserts (Corning) with 0.4 μm pores. Cells were submerged for the first 7 days in BEpiCM (ScienCell) with supplements, and then the apical medium was removed to establish an air-liquid interface that was maintained for the next 14 days. The basolateral medium was changed to differentiation medium containing a 1:1 mixture of DMEM (HyClone) and bronchial epithelial cell growth medium (BEGM; Lonza) with supplements and 50 nM all-trans retinoic acid (Sigma-Aldrich). Cells were stimulated with HDM (50 μg/ml; Greer Laboratories) and transfected with control or miR-206 mimic, control or miR-206 inhibitor

(RiboBio), scrambled or CD39 siRNA, and an empty or CD39 cDNA expression vector. Cells were also stimulated with HDM with or without apyrase or ATPγS (Sigma-Aldrich). BEAS-2B cell lines were purchased from ATCC (Manassas, VA). Cells were cultured in DMEM medium with 10% FBS and stimulated with Alternaria (50 μg/ml; Greer Laboratories) with or without apyrase.

Mouse model of allergic airway inflammation

Female C57BL/6 mice were obtained from the Experimental Animal Center of Hubei Province (Wuhan, China). The model was established by HDM sensitization and challenge. Briefly, female C57BL/6 mice received an intraperitoneal injection of 100 μl of a solution of lyophilized HDM extract (0.1 mg/ml; Greer Laboratories) and $Al(OH)_3$ as an adjuvant on days 0, 7 and 14, and received 40 μl of HDM solution (3 mg/ml) or saline intranasally on days 21, 22, and 23. miR-206 agomir (5 nmol in 40 μl saline; RiboBio), or control agomir, miR-206 antagomir (20 nmol in 40 μl saline) or control antagomir was administered intranasally on days 20 and 22. Twenty-four hours after the last HDM challenge, respiratory resistance in response to a range of concentrations of intravenous acetylcholine was measured using the forced oscillation technique with the FlexiVent system (SCIREQ) as previously described (73).

Assessment of mouse airway inflammation

Cell counts for macrophages, eosinophils, lymphocytes, and neutrophils in bronchoalveolar lavage fluid were performed as previously described (73). Paraffin-embedded 5-μm lung sections were stained with hematoxylin and eosin. The severity of peribronchial inflammation was scored by a blinded observer using the following features: 0, normal; 1, few cells; 2, a ring of inflammatory cells 1 cell layer deep; 3, a ring of inflammatory cells 2–4 cells deep; 4, a ring of

inflammatory cells >4 cells deep.

Immunohistochemistry

Sections of mouse lungs were stained with rabbit polyclonal CD39 (ENTPD1) antibody (Proteintech). Antibodies were detected using the Real EnVision detection system (Dako Diagnostics) according to the instructions.

PAS staining

Mouse lung sections were stained with periodic acid-Schiff (PAS) (Goodbio Technology) for detection of mucus. The number of PAS-positive cells was counted in four random fields for each lung section at ×200 magnification.

Quantitative polymerase chain reaction (PCR)

For quantification of hsa-miR-206 in epithelial brushings and HBE cells, mmu-miR-206 expression in mouse lungs; *CD39*, *IL-25*, *IL-33* (transcript without exons 3 and 4), *TSLP* (long isoform), *CLCA1*, *POSTN* and *SERPINB2* mRNA expression in epithelial brushings; and *Cd39* mRNA expression in mouse lungs, total RNA was isolated and reverse transcribed. Quantitative PCR was performed using an ABI Prism 7500 HT Fast Real-time PCR System (Applied Biosystems). The cycle threshold (Ct) of each gene transcript was normalized to the Ct of U6 or U48 for miRNA and to *β-actin* or *GAPDH* for mRNA. Relative gene expression was calculated using the 2(-Delta Delta Ct) method (74). The transcript levels of each gene are expressed as relative to the median level in healthy control subjects or the mean of the control group and log2 transformed. Primers for quantitative PCR are listed in the Supplementary Table. The stem-loop RT primer (ssD809230234), forward primer (ssD809230926) and reverse primer (ssD089261711) for hsa-/mmu-miR-206 were from RiboBio. TaqMan primer and probe sets for *IL25*

(Hs00224471_m1), *TSLP* (long isoform; Hs01572933_m1), and *ACTB* (Hs99999903_m1) were obtained from Applied Biosystems. The transcripts for *IL33* without exons 3 and 4 were determined by RNase H-dependent quantitative RT-PCR as reported by Gordon et al (48).

In situ hybridization

We performed in situ hybridization of mmu-miR-206 on paraffin-embedded sections using mmu-miR-206 miRCURY LNA miRNA detection probe (Qiagen). The sequence of the probes for mmu-miR-206 was 5'- CCACACACTTCCTTACATTCCA -3'.

Luciferase activity assay

BEAS-2B cells were co-transfected with vector harboring the wild-type, mutant *CD39* 3'-UTR or no 3'-UTR (control) and with miR-206 mimic or nontargeting control. Luciferase activity was detected with a dual luciferase reporter assay system (Promega). Normalized relative light units represent firefly luciferase activity/Renilla luciferase activity.

Western blotting

CD39 protein expression in cells was detected with monoclonal mouse-anti-human CD39 antibody (clone OTI2B10, OriGene Technologies) using Western blotting as previously described (73).

ELISA

Human IL-25 (RayBiotech), IL-33, and TSLP (R&D Systems) in supernatant from BALF and cell culture medium, and mouse Il-4, Il-5, Il-13 (R&D Systems), Il-25, Il-33 (Thermo Fisher Scientific), and Tslp (R&D Systems) in BALF supernatant were measured via ELISA according to the manufacturer's instructions. Mouse plasma IgE levels were determined via ELISA (Dakewe Biotech. All samples and standards were measured in duplicate.

ATP measurements

To measure ATP levels in human BALF, ice-cold BALF samples were centrifuged at 4℃ immediately after collection and the supernatants were stored at –80℃. Supernatants of fresh mouse BALF and cell culture medium were analyzed immediately. ATP levels were measured using an ATP assay kit (Beyotime Biotechnology) according to the instructions.

Flow cytometry

To analyze lung ILC2s, single-cell suspensions of mouse lung tissue were incubated with cocktail of biotin-conjugated monoclonal antibodies to detect lineage markers [CD5, CD11b, CD45R (B220), Anti-Gr-1 (Ly-6G/C), 7-4, and Ter-119] and then mixed with Anti-Biotin MicroBeads (Miltenyi Biotec). Lineage-negative lung cells were isolated with a column placed in the magnetic field of a MACS Separator (Miltenyi Biotec). Lineage-negative cells were stained with BV421-conjugated Live/Dead Fixable Dead Cell Stain (Invitrogen), PerCP/Cy5.5-conjugated CD25 (clone PC61; Biolegend), PE-conjugated CD127 (clone A7R34; Biolegend), FITC-conjugated T1/ST2 (clone DJ8; MD bioscience), and APC-conjugated Sca-1 (clone D7; Biolegend) antibodies. The samples were analyzed using an EPICS-XL MCL flow cytometer (Beckman Coulter). Live lineage-negative $CD25^{+}CD127^{+}T1/ST2^{+}Sca\text{-}1^{+}$ lymphocytes were identified as ILC2s. Data were analyzed with FlowJo software (TreeStar).

Statistics

We analyzed data using Prism version 5 (GraphPad Software) and SPSS version 19 (SPSS Inc.). For normally distributed data, we calculated the means ± standard deviation (SD) and used parametric tests (unpaired Student's *t* test or one-way ANOVA with Bonferroni's post hoc test). For nonnormally distributed data, we calculated the medians (with interquartile ranges) and used

nonparametric tests (Mann-Whitney test or one-way ANOVA with Bonferroni's post hoc test). We analyzed correlations using Spearman's rank order correlation. Values of $P < 0.05$ were considered statistically significant.

Study approvals

Human and mouse studies were approved by the ethics committee of Tongji Hospital, Tongji Medical College, Huazhong University of Science and Technology. Participants gave informed consent.

Author contributions: G.Z. designed the research, conceived of the manuscript and had primary responsibility for writing. K.Z., Y.F., Y.L., W.W., C.C., D.C., S.C., J.G., and G.C. performed experiments. K.Z., Y.F., Y.L., L.Y., D.C., and G.Z. analyzed data. K.Z., Y.F., Y.L., L.Y., D.C., and G.Z. interpreted results of experiments. K.Z., Y.F., and G.Z. prepared figures and drafted manuscript. G.Z. edited and revised manuscript. All authors reviewed and approved the manuscript.

Funding: This work was supported by National Natural Science Foundation of China (grant 91742108, 81670019, 81800026, 81600023), National Key Research and Development Program of China (2016YFC1304400), and Hubei Province Natural Science Foundation (grant 2017CFA016).

Acknowledgements: The authors thank all participants in this study; Xiaoling Rao and Mei Liu for bronchoscopy support; Wang Ni, Shixin Chen and Kun Zhang for spirometry measurement.

REFERENCES

1. Wenzel SE. Asthma phenotypes: the evolution from clinical to molecular approaches. *Nat Med.* 2012;18(5):716-25.
2. Agache I, and Akdis CA. Precision medicine and phenotypes, endotypes, genotypes, regiotypes, and theratypes of allergic diseases. *J Clin Invest.* 2019;129(4):1493-503.
3. Woodruff PG, Modrek B, Choy DF, Jia G, Abbas AR, Ellwanger A, et al. T-helper type 2-driven inflammation defines major subphenotypes of asthma. *Am J Respir Crit Care Med.* 2009;180(5):388-95.
4. Peebles RS, Jr., and Aronica MA. Proinflammatory Pathways in the Pathogenesis of Asthma. *Clin Chest Med.* 2019;40(1):29-50.
5. Hammad H, and Lambrecht BN. Barrier Epithelial Cells and the Control of Type 2 Immunity. *Immunity.* 2015;43(1):29-40.
6. Roan F, Obata-Ninomiya K, and Ziegler SF. Epithelial cell-derived cytokines: more than just signaling the alarm. *J Clin Invest.* 2019;129(4):1441-51.
7. Hiemstra PS, McCray PB, Jr., and Bals R. The innate immune function of airway epithelial cells in inflammatory lung disease. *Eur Respir J.* 2015;45(4):1150-62.
8. Fort MM, Cheung J, Yen D, Li J, Zurawski SM, Lo S, et al. IL-25 induces IL-4, IL-5, and IL-13 and Th2-associated pathologies in vivo. *Immunity.* 2001;15(6):985-95.
9. Schmitz J, Owyang A, Oldham E, Song Y, Murphy E, McClanahan TK, et al. IL-33, an interleukin-1-like cytokine that signals via the IL-1 receptor-related protein ST2 and induces T helper type 2-associated cytokines. *Immunity.* 2005;23(5):479-90.
10. Soumelis V, Reche PA, Kanzler H, Yuan W, Edward G, Homey B, et al. Human epithelial cells trigger dendritic cell mediated allergic inflammation by producing TSLP. *Nat Immunol.* 2002;3(7):673-80.
11. Al-Shami A, Spolski R, Kelly J, Keane-Myers A, and Leonard WJ. A role for TSLP in the development of inflammation in an asthma model. *J Exp Med.* 2005;202(6):829-39.
12. Bloodworth MH, Rusznak M, Pfister CC, Zhang J, Bastarache L, Calvillo SA, et al. Glucagon-like peptide 1 receptor signaling attenuates respiratory syncytial virus-induced type 2 responses and immunopathology. *J Allergy Clin Immunol.* 2018;142(2):683-7 e12.
13. Vercelli D. When Innate Responses Matter: ILC2s Loom Large in Allergic Airway Inflammation. *Am J Respir Crit Care Med.* 2017;195(12):1544-6.
14. Causton B, Pardo-Saganta A, Gillis J, Discipio K, Kooistra T, Rajagopal J, et al. CARMA3 Mediates Allergic Lung Inflammation in Response to Alternaria alternata. *Am J Respir Cell Mol Biol.* 2018;59(6):684-94.
15. Altman MC, Lai Y, Nolin JD, Long S, Chen CC, Piliponsky AM, et al. Airway epithelium-shifted mast cell infiltration regulates asthmatic inflammation via IL-33 signaling. *J Clin Invest.* 2019;129(11):4979-91.
16. Wang YH, Angkasekwinai P, Lu N, Voo KS, Arima K, Hanabuchi S, et al. IL-25 augments type 2 immune responses by enhancing the expansion and functions of TSLP-DC-activated Th2 memory cells. *J Exp Med.* 2007;204(8):1837-47.
17. Endo Y, Hirahara K, Iinuma T, Shinoda K, Tumes DJ, Asou HK, et al. The interleukin-33-p38 kinase axis confers memory T helper 2 cell pathogenicity in the airway. *Immunity.* 2015;42(2):294-308.
18. Ballantyne SJ, Barlow JL, Jolin HE, Nath P, Williams AS, Chung KF, et al. Blocking IL-25 prevents airway hyperresponsiveness in allergic asthma. *J Allergy Clin Immunol.* 2007;120(6):1324-31.
19. Suzukawa M, Morita H, Nambu A, Arae K, Shimura E, Shibui A, et al. Epithelial cell-derived IL-25, but not Th17 cell-derived IL-17 or IL-17F, is crucial for murine asthma. *J Immunol.* 2012;189(7):3641-52.
20. Liew FY, Pitman NI, and McInnes IB. Disease-associated functions of IL-33: the new kid in the IL-1 family. *Nat*

Rev Immunol. 2010;10(2):103-10.

21. Lee JU, Chang HS, Lee HJ, Bae DJ, Son JH, Park JS, et al. Association of interleukin-25 levels with development of aspirin induced respiratory diseases. *Respir Med.* 2017;123:71-8.

22. Seys SF, Grabowski M, Adriaensen W, Decraene A, Dilissen E, Vanoirbeek JA, et al. Sputum cytokine mapping reveals an 'IL-5, IL-17A, IL-25-high' pattern associated with poorly controlled asthma. *Clin Exp Allergy.* 2013;43(9):1009-17.

23. Li Y, Wang W, Lv Z, Chen Y, Huang K, Corrigan CJ, et al. Elevated Expression of IL-33 and TSLP in the Airways of Human Asthmatics In Vivo: A Potential Biomarker of Severe Refractory Disease. *J Immunol.* 2018;200(7):2253-62.

24. Gluck J, Rymarczyk B, Kasprzak M, and Rogala B. Increased Levels of Interleukin-33 and Thymic Stromal Lymphopoietin in Exhaled Breath Condensate in Chronic Bronchial Asthma. *Int Arch Allergy Immunol.* 2016;169(1):51-6.

25. Bleck B, Kazeros A, Bakal K, Garcia-Medina L, Adams A, Liu M, et al. Coexpression of type 2 immune targets in sputum-derived epithelial and dendritic cells from asthmatic subjects. *J Allergy Clin Immunol.* 2015;136(3):619-27 e5.

26. O'Grady SM, Patil N, Melkamu T, Maniak PJ, Lancto C, and Kita H. ATP release and Ca2+ signalling by human bronchial epithelial cells following Alternaria aeroallergen exposure. *J Physiol.* 2013;591(18):4595-609.

27. Kool M, Willart MA, van Nimwegen M, Bergen I, Pouliot P, Virchow JC, et al. An unexpected role for uric acid as an inducer of T helper 2 cell immunity to inhaled antigens and inflammatory mediator of allergic asthma. *Immunity.* 2011;34(4):527-40.

28. Idzko M, Hammad H, van Nimwegen M, Kool M, Willart MA, Muskens F, et al. Extracellular ATP triggers and maintains asthmatic airway inflammation by activating dendritic cells. *Nat Med.* 2007;13(8):913-9.

29. Picher M, Burch LH, Hirsh AJ, Spychala J, and Boucher RC. Ecto 5'-nucleotidase and nonspecific alkaline phosphatase. Two AMP-hydrolyzing ectoenzymes with distinct roles in human airways. *J Biol Chem.* 2003;278(15):13468-79.

30. Leal DB, Streher CA, Neu TN, Bittencourt FP, Leal CA, da Silva JE, et al. Characterization of NTPDase (NTPDase1; ecto-apyrase; ecto-diphosphohydrolase; CD39; EC 3.6.1.5) activity in human lymphocytes. *Biochim Biophys Acta.* 2005;1721(1-3):9-15.

31. Chavez J, Vargas MH, Rebollar-Ayala DC, Diaz-Hernandez V, Cruz-Valderrama JE, Flores-Soto E, et al. Inhibition of extracellular nucleotides hydrolysis intensifies the allergic bronchospasm. A novel protective role of ectonucleotidases. *Allergy.* 2013;68(4):462-71.

32. Li P, Gao Y, Cao J, Wang W, Chen Y, Zhang G, et al. CD39+ regulatory T cells attenuate allergic airway inflammation. *Clin Exp Allergy.* 2015;45(6):1126-37.

33. Idzko M, C KA, Muller T, Durk T, Grimm M, Baudiss K, et al. Attenuated allergic airway inflammation in Cd39 null mice. *Allergy.* 2013;68(4):472-80.

34. Kouzaki H, Iijima K, Kobayashi T, O'Grady SM, and Kita H. The danger signal, extracellular ATP, is a sensor for an airborne allergen and triggers IL-33 release and innate Th2-type responses. *J Immunol.* 2011;186(7):4375-87.

35. Baumjohann D, and Ansel KM. MicroRNA-mediated regulation of T helper cell differentiation and plasticity. *Nat Rev Immunol.* 2013;13(9):666-78.

36. Solberg OD, Ostrin EJ, Love MI, Peng JC, Bhakta NR, Hou L, et al. Airway epithelial miRNA expression is altered in asthma. *Am J Respir Crit Care Med.* 2012;186(10):965-74.

37. Singh PB, Pua HH, Happ HC, Schneider C, von Moltke J, Locksley RM, et al. MicroRNA regulation of type 2 innate lymphoid cell homeostasis and function in allergic inflammation. *J Exp Med.* 2017;214(12):3627-43.

38. Simpson LJ, Patel S, Bhakta NR, Choy DF, Brightbill HD, Ren X, et al. A microRNA upregulated in asthma airway T cells promotes TH2 cytokine production. *Nat Immunol.* 2014;15(12):1162-70.
39. Polikepahad S, Knight JM, Naghavi AO, Oplt T, Creighton CJ, Shaw C, et al. Proinflammatory role for let-7 microRNAS in experimental asthma. *J Biol Chem.* 2010;285(39):30139-49.
40. Kumar M, Ahmad T, Sharma A, Mabalirajan U, Kulshreshtha A, Agrawal A, et al. Let-7 microRNA-mediated regulation of IL-13 and allergic airway inflammation. *J Allergy Clin Immunol.* 2011;128(5):1077-85 e1-10.
41. Huo X, Zhang K, Yi L, Mo Y, Liang Y, Zhao J, et al. Decreased epithelial and plasma miR-181b-5p expression associates with airway eosinophilic inflammation in asthma. *Clin Exp Allergy.* 2016;46(10):1281-90.
42. Bhakta NR, Solberg OD, Nguyen CP, Nguyen CN, Arron JR, Fahy JV, et al. A qPCR-based metric of Th2 airway inflammation in asthma. *Clin Transl Allergy.* 2013;3(1):24.
43. Tasena H, Boudewijn IM, Faiz A, Timens W, Hylkema MN, Berg M, et al. MiR-31-5p: A shared regulator of chronic mucus hypersecretion in asthma and chronic obstructive pulmonary disease. *Allergy.* 2020;75(3):703-6.
44. Comer BS, Camoretti-Mercado B, Kogut PC, Halayko AJ, Solway J, and Gerthoffer WT. MicroRNA-146a and microRNA-146b expression and anti-inflammatory function in human airway smooth muscle. *Am J Physiol Lung Cell Mol Physiol.* 2014;307(9):L727-34.
45. Perry MM, Baker JE, Gibeon DS, Adcock IM, and Chung KF. Airway smooth muscle hyperproliferation is regulated by microRNA-221 in severe asthma. *Am J Respir Cell Mol Biol.* 2014;50(1):7-17.
46. Zhang K, Liang Y, Feng Y, Wu W, Zhang H, He J, et al. Decreased epithelial and sputum miR-221-3p associates with airway eosinophilic inflammation and CXCL17 expression in asthma. *Am J Physiol Lung Cell Mol Physiol.* 2018;315(2):L253-L64.
47. Burch LH, and Picher M. E-NTPDases in human airways: Regulation and relevance for chronic lung diseases. *Purinergic signalling.* 2006;2(2):399-408.
48. Gordon ED, Simpson LJ, Rios CL, Ringel L, Lachowicz-Scroggins ME, Peters MC, et al. Alternative splicing of interleukin-33 and type 2 inflammation in asthma. *Proc Natl Acad Sci U S A.* 2016;113(31):8765-70.
49. Fornasa G, Tsilingiri K, Caprioli F, Botti F, Mapelli M, Meller S, et al. Dichotomy of short and long thymic stromal lymphopoietin isoforms in inflammatory disorders of the bowel and skin. *J Allergy Clin Immunol.* 2015;136(2):413-22.
50. Lu TX, Munitz A, and Rothenberg ME. MicroRNA-21 is up-regulated in allergic airway inflammation and regulates IL-12p35 expression. *J Immunol.* 2009;182(8):4994-5002.
51. Malmhall C, Alawieh S, Lu Y, Sjostrand M, Bossios A, Eldh M, et al. MicroRNA-155 is essential for T(H)2-mediated allergen-induced eosinophilic inflammation in the lung. *J Allergy Clin Immunol.* 2014;133(5):1429-38, 38 e1-7.
52. Collison A, Siegle JS, Hansbro NG, Kwok CT, Herbert C, Mattes J, et al. Epigenetic changes associated with disease progression in a mouse model of childhood allergic asthma. *Dis Model Mech.* 2013;6(4):993-1000.
53. Lin CC, Law BF, Siegel PD, and Hettick JM. Circulating miRs-183-5p, -206-3p and -381-3p may serve as novel biomarkers for 4,4'-methylene diphenyl diisocyanate exposure. *Biomarkers.* 2019;24(1):76-90.
54. Lin CC, Law BF, and Hettick JM. Acute 4,4'-Methylene Diphenyl Diisocyanate Exposure-Mediated Downregulation of miR-206-3p and miR-381-3p Activates Inducible Nitric Oxide Synthase Transcription by Targeting Calcineurin/NFAT Signaling in Macrophages. *Toxicol Sci.* 2020;173(1):100-13.
55. Kho AT, McGeachie MJ, Moore KG, Sylvia JM, Weiss ST, and Tantisira KG. Circulating microRNAs and prediction of asthma exacerbation in childhood asthma. *Respir Res.* 2018;19(1):128.
56. Panganiban RP, Wang Y, Howrylak J, Chinchilli VM, Craig TJ, August A, et al. Circulating microRNAs as biomarkers in patients with allergic rhinitis and asthma. *J Allergy Clin Immunol.* 2016;137(5):1423-32.

57. Beccafico S, Morozzi G, Marchetti MC, Riccardi C, Sidoni A, Donato R, et al. Artesunate induces ROS- and p38 MAPK-mediated apoptosis and counteracts tumor growth in vivo in embryonal rhabdomyosarcoma cells. *Carcinogenesis.* 2015;36(9):1071-83.
58. Climent M, Viggiani G, Chen YW, Coulis G, and Castaldi A. MicroRNA and ROS Crosstalk in Cardiac and Pulmonary Diseases. *Int J Mol Sci.* 2020;21(12).
59. Dickinson JD, Alevy Y, Malvin NP, Patel KK, Gunsten SP, Holtzman MJ, et al. IL13 activates autophagy to regulate secretion in airway epithelial cells. *Autophagy.* 2016;12(2):397-409.
60. Leung TF, To MY, Yeung AC, Wong YS, Wong GW, and Chan PK. Multiplex molecular detection of respiratory pathogens in children with asthma exacerbation. *Chest.* 2010;137(2):348-54.
61. Calven J, Akbarshahi H, Menzel M, Ayata CK, Idzko M, Bjermer L, et al. Rhinoviral stimuli, epithelial factors and ATP signalling contribute to bronchial smooth muscle production of IL-33. *J Transl Med.* 2015;13:281.
62. Wolk KE, Lazarowski ER, Traylor ZP, Yu EN, Jewell NA, Durbin RK, et al. Influenza A virus inhibits alveolar fluid clearance in BALB/c mice. *Am J Respir Crit Care Med.* 2008;178(9):969-76.
63. Cheng D, Xue Z, Yi L, Shi H, Zhang K, Huo X, et al. Epithelial interleukin-25 is a key mediator in Th2-high, corticosteroid-responsive asthma. *Am J Respir Crit Care Med.* 2014;190(6):639-48.
64. Shin HW, Kim DK, Park MH, Eun KM, Lee M, So D, et al. IL-25 as a novel therapeutic target in nasal polyps of patients with chronic rhinosinusitis. *J Allergy Clin Immunol.* 2015;135(6):1476-85 e7.
65. Iinuma T, Okamoto Y, Yamamoto H, Inamine-Sasaki A, Ohki Y, Sakurai T, et al. Interleukin-25 and mucosal T cells in noneosinophilic and eosinophilic chronic rhinosinusitis. *Ann Allergy Asthma Immunol.* 2015;114(4):289-98.
66. Chen F, Hong H, Sun Y, Hu X, Zhang J, Xu G, et al. Nasal interleukin 25 as a novel biomarker for patients with chronic rhinosinusitis with nasal polyps and airway hypersensitiveness: A pilot study. *Ann Allergy Asthma Immunol.* 2017;119(4):310-6 e2.
67. Ogasawara N, Klingler AI, Tan BK, Poposki JA, Hulse KE, Stevens WW, et al. Epithelial activators of type 2 inflammation: Elevation of thymic stromal lymphopoietin, but not IL-25 or IL-33, in chronic rhinosinusitis with nasal polyps in Chicago, Illinois. *Allergy.* 2018;73(11):2251-4.
68. Miljkovic D, Bassiouni A, Cooksley C, Ou J, Hauben E, Wormald PJ, et al. Association between group 2 innate lymphoid cells enrichment, nasal polyps and allergy in chronic rhinosinusitis. *Allergy.* 2014;69(9):1154-61.
69. Ozturan A, Eyigor H, Eyigor M, Osma U, Yilmaz MD, Selcuk OT, et al. The role of IL-25 and IL-33 in chronic rhinosinusitis with or without nasal polyps. *Eur Arch Otorhinolaryngol.* 2017;274(1):283-8.
70. Olejniczak M, Galka P, and Krzyzosiak WJ. Sequence-non-specific effects of RNA interference triggers and microRNA regulators. *Nucleic Acids Res.* 2010;38(1):1-16.
71. Kelsen SG, Mardini IA, Zhou S, Benovic JL, and Higgins NC. A technique to harvest viable tracheobronchial epithelial cells from living human donors. *Am J Respir Cell Mol Biol.* 1992;7(1):66-72.
72. Zhen G, Park SW, Nguyenvu LT, Rodriguez MW, Barbeau R, Paquet AC, et al. IL-13 and epidermal growth factor receptor have critical but distinct roles in epithelial cell mucin production. *Am J Respir Cell Mol Biol.* 2007;36(2):244-53.
73. Yi L, Cheng D, Zhang K, Huo X, Mo Y, Shi H, et al. Intelectin contributes to allergen-induced IL-25, IL-33, and TSLP expression and type 2 response in asthma and atopic dermatitis. *Mucosal Immunol.* 2017;10(6):1491-503.
74. Livak KJ, and Schmittgen TD. Analysis of relative gene expression data using real-time quantitative PCR and the 2(-Delta Delta C(T)) Method. *Methods.* 2001;25(4):402-8.

Figure 1

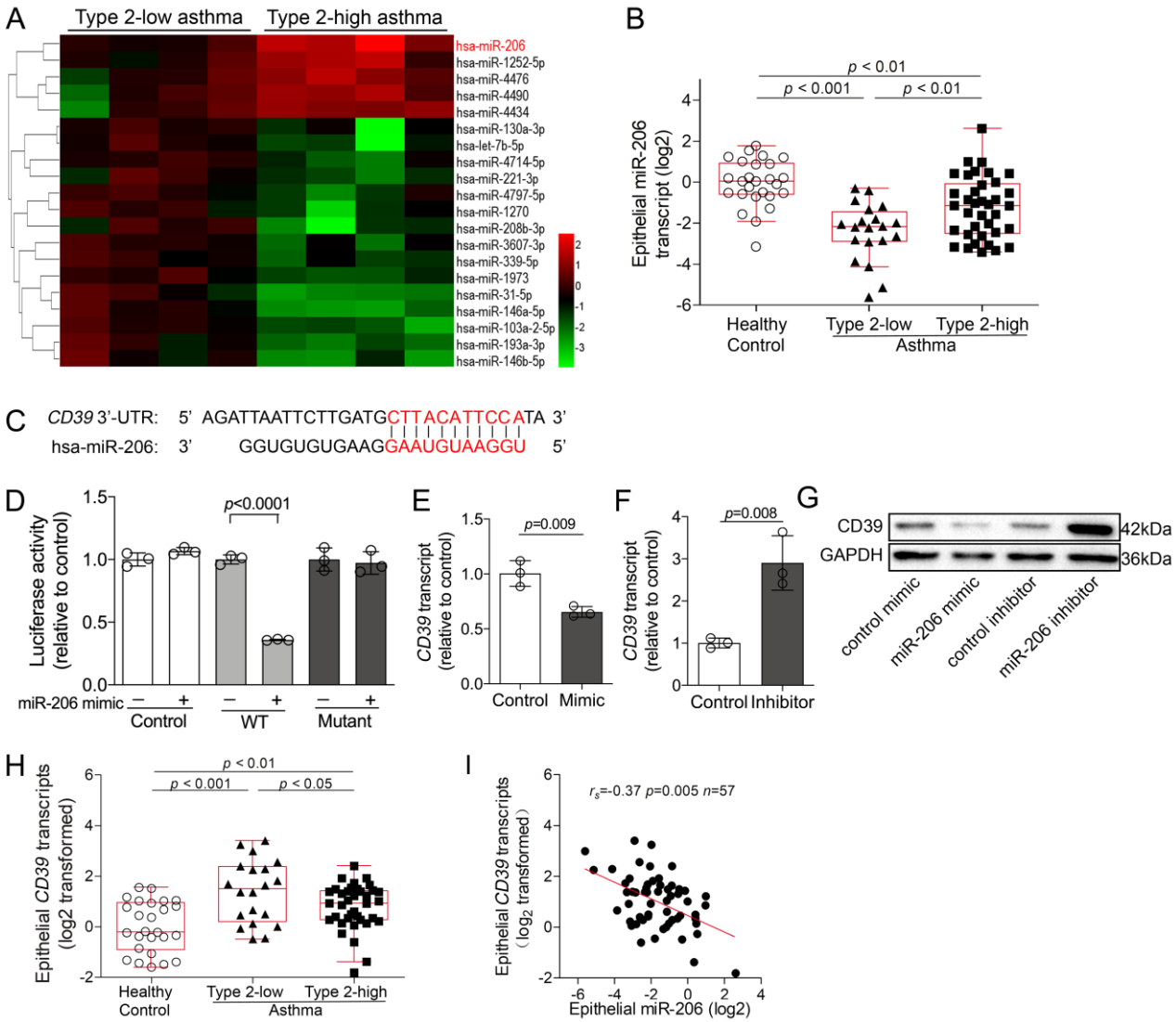
A
Type 2-low asthma
Type 2-high asthma
hsa-miR-206
hsa-miR-1252-5p
hsa-miR-4476
hsa-miR-4490
hsa-miR-4434
hsa-miR-130a-3p
hsa-let-7b-5p
hsa-miR-4714-5p
hsa-miR-221-3p
hsa-miR-4797-5p
hsa-miR-1270
hsa-miR-208b-3p
hsa-miR-3607-3p
hsa-miR-339-5p
hsa-miR-1973
hsa-miR-31-5p
hsa-miR-146a-5p
hsa-miR-103a-2-5p
hsa-miR-193a-3p
hsa-miR-146b-5p
B
p < 0.01
p < 0.001
p < 0.01
Epithelial miR-206 transcript (log2)
Healthy Control
Type 2-low
Type 2-high
Asthma
C
CD39 3'-UTR: 5' AGATTAATTCTTGATGCTTACATTCCATA 3'
hsa-miR-206: 3' GGUGUGUGAAGGAAUGUAAGGU 5'
D
p<0.0001
Luciferase activity (relative to control)
miR-206 mimic
Control
WT
Mutant
E
p=0.009
CD39 transcript (relative to control)
Control
Mimic
F
p=0.008
CD39 transcript (relative to control)
Control
Inhibitor
G
CD39
GAPDH
42kDa
36kDa
control mimic
miR-206 mimic
control inhibitor
miR-206 inhibitor
H
p < 0.01
p < 0.001
p < 0.05
Epithelial CD39 transcripts (log2 transformed)
Healthy Control
Type 2-low
Type 2-high
Asthma
I
rs=-0.37 p=0.005 n=57
Epithelial CD39 transcripts (log2 transformed)
Epithelial miR-206 (log2)

Figure 1. An epithelial miRNA differentially expressed between type 2-low and type 2-high asthma, miR-206, targets CD39. (A) Twenty differentially expressed epithelial miRNAs between subjects with type 2-low asthma (n = 4) and type 2-high asthma (n = 4) were identified using microarrays. Each column represents data from one subject. Colors represent fold change relative to the mean value of type 2-low asthma. (B) miR-206 transcript levels in bronchial brushings from healthy controls (n = 26), type 2-low (n = 20) and type 2-high asthma patients (n = 37) were determined by quantitative PCR. The transcript levels are relative to the median of healthy controls and log2 transformed. Data represent medians with interquartile ranges (one-way ANOVA with Bonferroni's post hoc test). (C) The 3'-UTR of *CD39* contains a region that matches the seed sequence of hsa-miR-206. (D) 3'-UTR luciferase reporter assay with vector harboring wild-type (WT), mutant *CD39* 3'-UTR or no 3'-UTR (control) co-transfected with miR-206 mimic or nontargeting control. Luciferase activity was measured with a dual-luciferase reporter assay system. The firefly luciferase activity was normalized to Renilla luciferase activity. n = 3 per group. (E, F) *CD39* transcript levels in BEAS-2B cells after transfection with miR-206 mimic (*E*) or inhibitor (*F*) were determined by quantitative PCR. The transcript levels are relative to the mean value of control group (two-tailed Student's *t* test). n = 3 per group. The data are mean ± SD. (G) CD39 protein expression in BEAS-2B cells after transfection with miR-206 mimic and inhibitor was determined by Western blotting. (H) *CD39* transcript levels in bronchial brushings from healthy controls (n = 26), type 2-low asthma (n = 20) and type 2-high asthma patients (n=37) were determined by quantitative PCR. Data are expressed and compared as in Figure 1B. (I) Spearman's rank order correlation assay between epithelial *CD39* and miR-206 transcript levels in all asthma patients (n = 57).

Figure 2

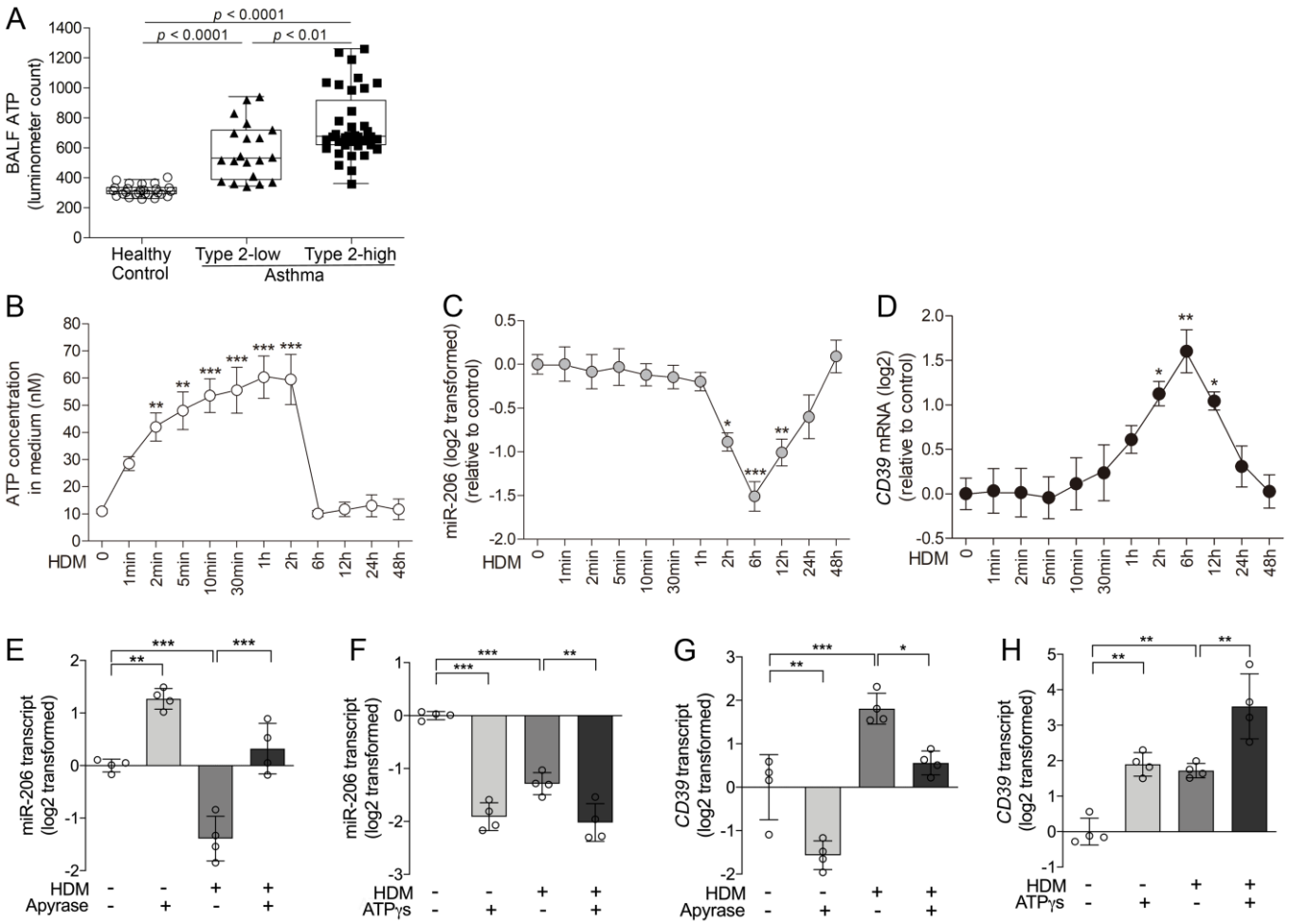
A
p < 0.0001
p < 0.0001
p < 0.01
BALF ATP (luminometer count)
Healthy Control
Type 2-low
Type 2-high
Asthma
B
ATP concentration in medium (nM)
HDM
C
miR-206 (log2 transformed) (relative to control)
D
CD39 mRNA (log2) (relative to control)
E
miR-206 transcript (log2 transformed)
HDM
Apyrase
F
miR-206 transcript (log2 transformed)
HDM
ATPγs
G
CD39 transcript (log2 transformed)
HDM
Apyrase
H
CD39 transcript (log2 transformed)
HDM
ATPγs

Figure 2. Acute extracellular ATP accumulation is responsible for allergen-induced miR-206 downregulation and CD39 upregulation in bronchial epithelial cells. (A) ATP levels in BALF from healthy controls (n = 26), type 2-low (n = 20) and type 2-high asthma patients (n = 37) were determined by luciferase bioluminescence. Data are expressed as median values with interquartile ranges. The lines within the boxes represent medians, and the bounds of the boxes represent interquartile ranges. The whiskers are plotted using Tukey method. One-way ANOVA with Bonferroni's post hoc test was performed. (B) ATP concentration in culture medium collected at indicated time points after HDM stimulation was measured using luciferase bioluminescence. (C, D) Transcript levels of miR-206 (*C*) and *CD39* (*D*) in HBE cells harvested at the indicated time points after HDM stimulation were determined by quantitative PCR. n = 4 wells per time point combined from 2 experiments using HBE cells from 2 healthy donors. The data are mean ± SD. $*P < 0.05$; $**P < 0.01$; $***P < 0.001$ (one-way ANOVA with Bonferroni's post hoc test). (E-F) miR-206 transcript levels in HBE cells pretreated with apyrase or saline for 2 h before addition of HDM and stimulation for 6 h (*E*), and treated with ATPγS or saline with or without HDM for 6 h (*F*). (G, H) *CD39* transcript levels in HBE cells pretreated with apyrase or saline for 2 h before addition HDM and stimulation for 6 h (*G*), and treated with ATPγS or saline with or without HDM for 6h (*H*). The transcript levels are relative to the mean value of control group and log2 transformed. n = 4 wells per group combined from 2 experiments using HBE cells from 2 healthy donors. The data are mean ± SD. $*P < 0.05$; $**P < 0.01$; $***P < 0.001$ (one-way ANOVA with Bonferroni's post hoc test).

Figure 3

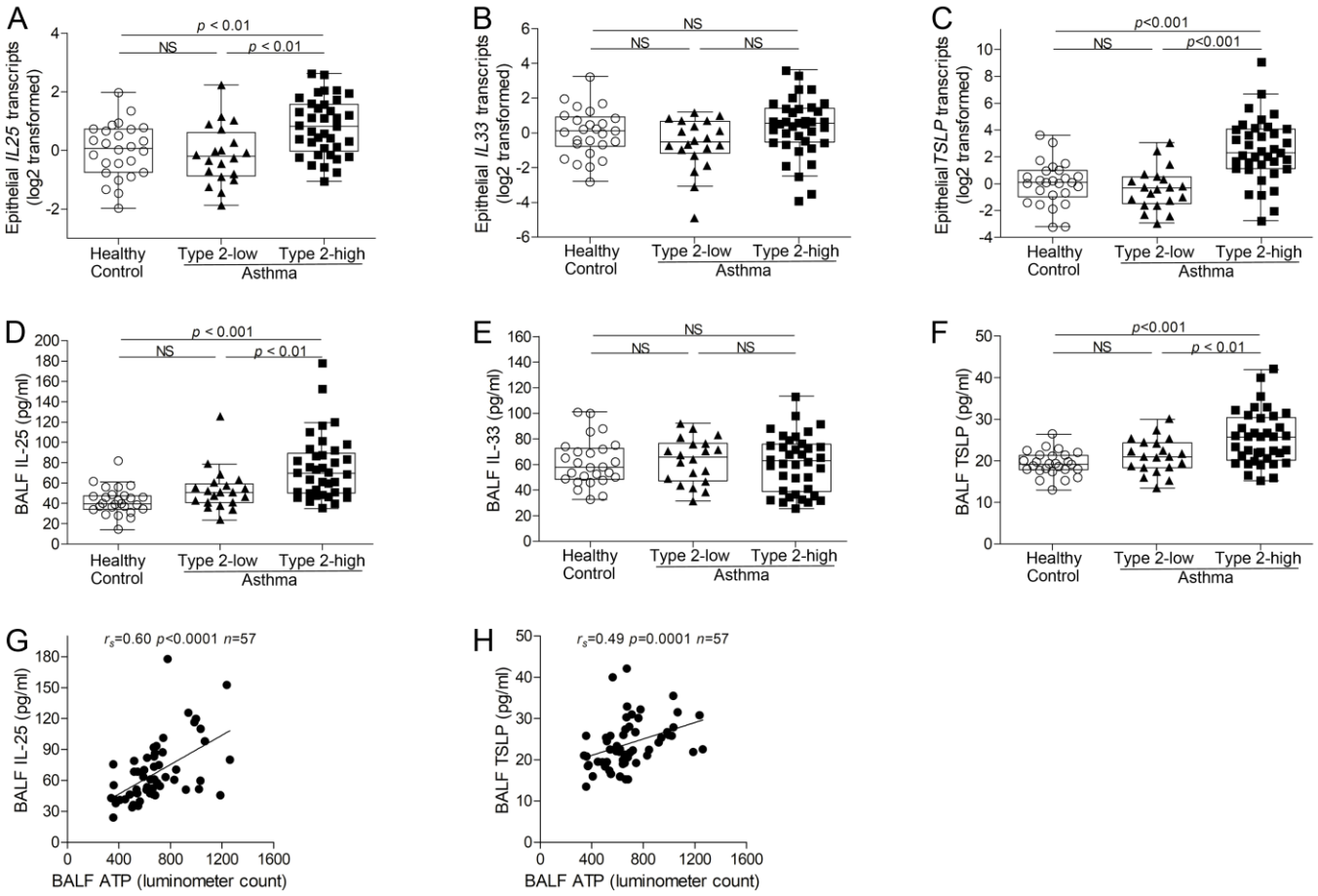
A
Epithelial IL25 transcripts (log2 transformed)
p < 0.01
NS
p < 0.01
Healthy Control
Type 2-low
Type 2-high
Asthma
B
Epithelial IL33 transcripts (log2 transformed)
NS
NS
NS
C
Epithelial TSLP transcripts (log2 transformed)
p<0.001
NS
p<0.001
D
BALF IL-25 (pg/ml)
p < 0.001
NS
p < 0.01
E
BALF IL-33 (pg/ml)
F
BALF TSLP (pg/ml)
G
rs=0.60 p<0.0001 n=57
BALF IL-25 (pg/ml)
BALF ATP (luminometer count)
H
rs=0.49 p=0.0001 n=57
BALF TSLP (pg/ml)
BALF ATP (luminometer count)

Figure 3. **Airway IL-25 and TSLP expression is elevated in type 2-high asthma and correlated with BALF ATP levels.** (A-C) The transcripts of *IL25* (*A*), *IL33* without exons 3 and 4 (*B*), and the long isoform of *TSLP* (*C*) in bronchial epithelial brushings from healthy controls (n = 26), type 2-low (n = 20) and type 2-high asthma patients (n = 37) were determined using quantitative PCR with TaqMan primers and probes. For detection of *IL33* transcripts without exons 3 and 4, RNase H-dependent quantitative PCR was performed. The transcript levels are relative to the median value of healthy controls and log2 transformed. (D-F) IL-25 (*D*), IL-33 (*E*) and TSLP (*F*) protein levels in BALF from healthy controls (n = 26), type 2-low (n = 20) and type 2-high asthma (n = 37) were determined using ELISA. Data are expressed as median values with interquartile ranges. The lines within the boxes represent medians, and the bounds of the boxes represent interquartile ranges. The whiskers are plotted using Tukey method. One-way ANOVA with Bonferroni's post hoc test was performed. (G-H) Spearman's rank order correlation assays between BALF ATP levels and BALF IL-25 protein levels (*G*) and TSLP protein levels (*H*).

Figure 4

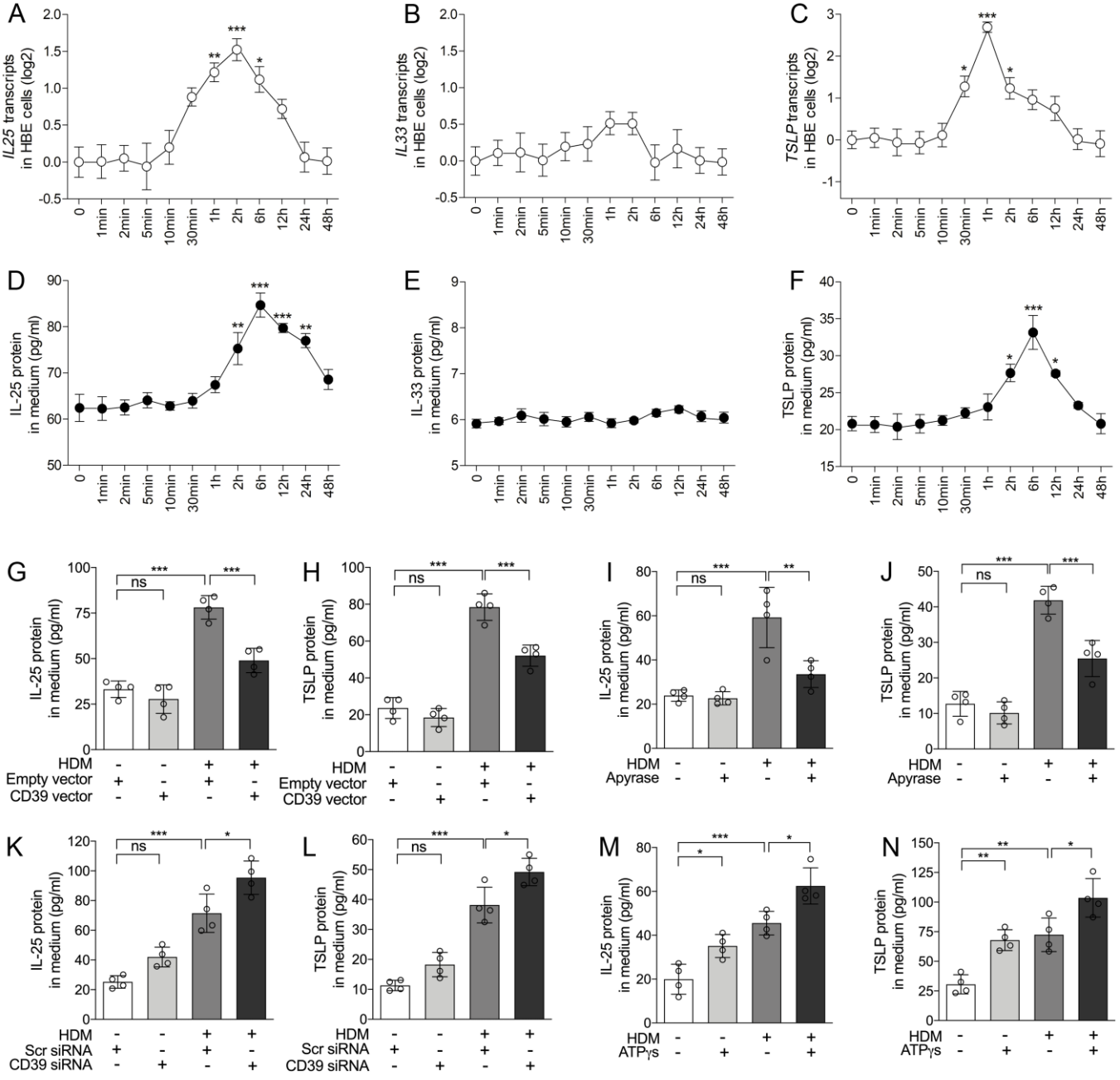
A
IL25 transcripts in HBE cells (log2)
B
IL33 transcripts in HBE cells (log2)
C
TSLP transcripts in HBE cells (log2)
D
IL-25 protein in medium (pg/ml)
E
IL-33 protein in medium (pg/ml)
F
TSLP protein in medium (pg/ml)
0 1min 2min 5min 10min 30min 1h 2h 6h 12h 24h 48h
G
IL-25 protein in medium (pg/ml)
H
TSLP protein in medium (pg/ml)
I
IL-25 protein in medium (pg/ml)
J
TSLP protein in medium (pg/ml)
HDM
Empty vector
CD39 vector
Apyrase
K
IL-25 protein in medium (pg/ml)
L
TSLP protein in medium (pg/ml)
M
IL-25 protein in medium (pg/ml)
N
TSLP protein in medium (pg/ml)
HDM
Scr siRNA
CD39 siRNA
ATPγs
ns

Figure 4. Extracellular ATP is required and sufficient for IL-25 and TSLP expression in bronchial epithelial cells. (A-C) The transcripts of *IL25* (*A*), *IL33* without exons 3 and 4 (*B*), and the long isoform of *TSLP* (*C*) in HBE cells harvested at the indicated time points after HDM stimulation were determined by quantitative PCR. (D-F) IL-25 (*D*), IL-33 (*E*) and TSLP (*F*) protein levels in culture medium collected at the indicated time points after HDM stimulation were determined using ELISAs. n = 4 wells per time points combined from 2 experiments using HBE cells from 2 healthy donors. Data are mean ± SD. **P* < 0.05; ***P* < 0.01; ****P* < 0.001 (one-way ANOVA with Bonferroni's post hoc test). (G, H) IL-25 (*G*) and TSLP (*H*) protein levels in culture medium after transfection with empty or CD39 expression vector and stimulation with or without HDM for 6 h were determined using ELISAs. (I, J) IL-25 (*I*) and TSLP (*J*) protein levels in culture medium after pretreatment with apyrase or saline and stimulation with or without HDM for 6 h were determined using ELISAs. (K, L) IL-25 (*K*) and TSLP (*L*) protein levels in culture medium after transfection with scrambled or CD39 siRNA and stimulation with or without HDM for 6 h were determined using ELISAs. (M, N) IL-25 (*M*) and TSLP (*N*) protein levels in culture medium after treatment with ATPγS or saline and with or without HDM for 6 h were determined using ELISAs. n = 4 wells per group combined from 2 experiments using HBE cells from 2 healthy donors. Data are mean ± SD. **P* < 0.05; ***P* < 0.01; ****P* < 0.001 (one-way ANOVA with Bonferroni's post hoc test).

Figure 5

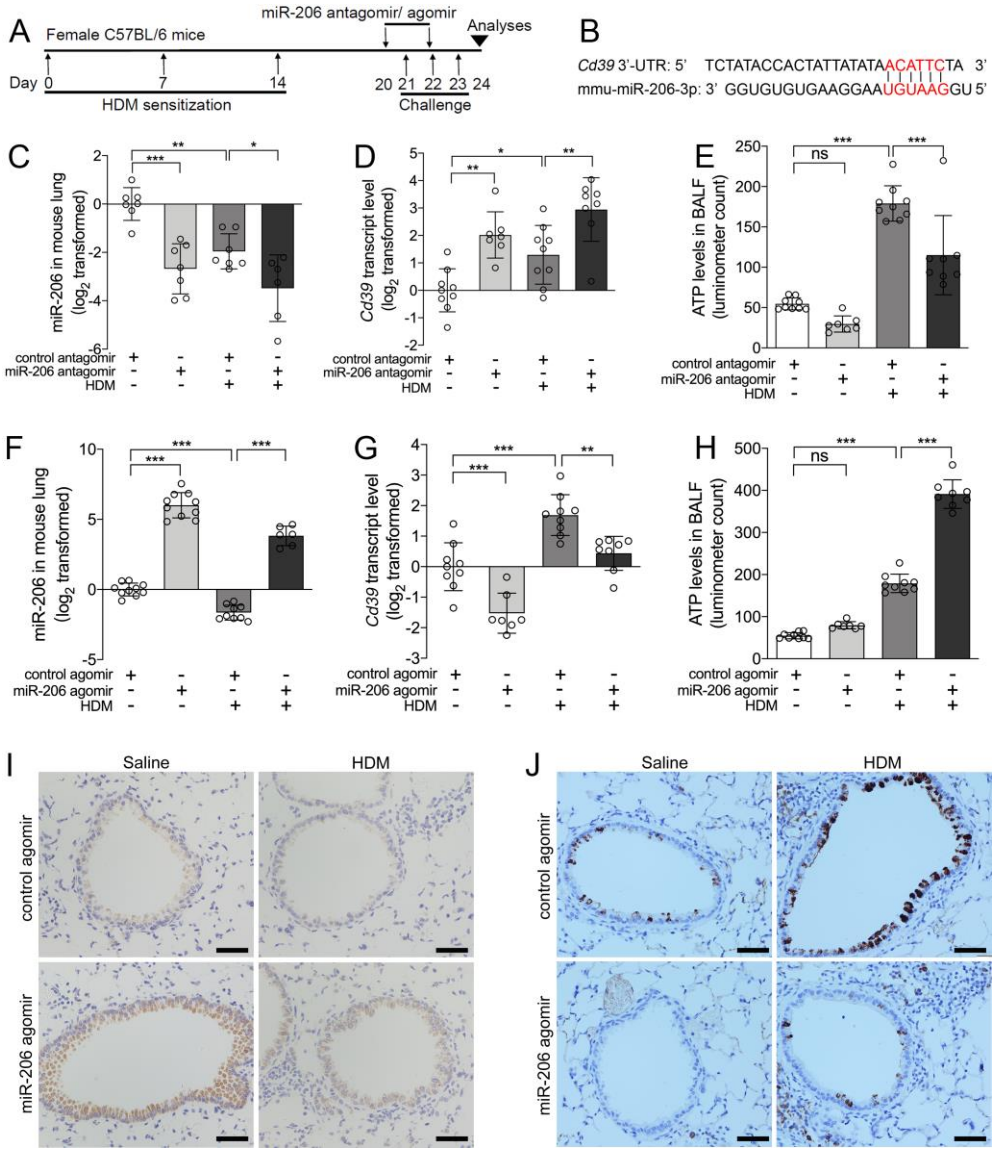
A
Female C57BL/6 mice
miR-206 antagomir/ agomir
Analyses
Day 0 7 14 20 21 22 23 24
HDM sensitization
Challenge
B
Cd39 3'-UTR: 5' TCTATACCACTATTATATAACATTCTA 3'
mmu-miR-206-3p: 3' GGUGUGUGAAGGAAUGUAAGGU 5'
C
miR-206 in mouse lung (log2 transformed)
control antagomir
miR-206 antagomir
HDM
D
Cd39 transcript level (log2 transformed)
E
ATP levels in BALF (luminometer count)
ns
F
miR-206 in mouse lung (log2 transformed)
control agomir
miR-206 agomir
G
Cd39 transcript level (log2 transformed)
H
ATP levels in BALF (luminometer count)
I
Saline
HDM
control agomir
miR-206 agomir
J
Saline
HDM
control agomir
miR-206 agomir

Figure 5. Epithelial miR-206 targets the CD39-extracellular ATP axis in a murine model of allergic airway inflammation. (A) Experimental schedule. (B) The seed region of *mmu-miR-206-3p,* and the seed recognizing sites in the 3'-UTR of mouse *Cd39* variant 1 (position 2864-2869) are shown. (C-E) miR-206 (*C*) and *Cd39* (*D*) transcript levels in the lungs, and ATP levels in BALF (*E*) were determined by quantitative PCR and luciferase bioluminescence, respectively, in mice intranasally administered control or miR-206 antagomir and challenged with HDM or saline. (F-H) miR-206 (*F*) and *Cd39* (*G*) transcript levels in the lungs, and ATP levels in BALF (*H*) were determined by quantitative PCR and luciferase bioluminescence, respectively, in mice intranasally administered control or miR-206 agomir and challenged with HDM or saline. The transcript levels are relative to the mean value of the control group and log2 transformed. n = 6 - 10 mice per group combined from 2 independent experiments. The data are mean ± SD. **P* < 0.05; ***P* < 0.01; ****P* < 0.001 (one-way ANOVA with Bonferroni's post hoc test). (I, J) Representative images of in situ hybridization of miR-206 (*I*), and immunohistochemistry of CD39 (*J*) in lung sections from mice intranasally administered control or miR-206 agomir and challenged with HDM or saline. Scale bar = 50 μm.

Figure 6

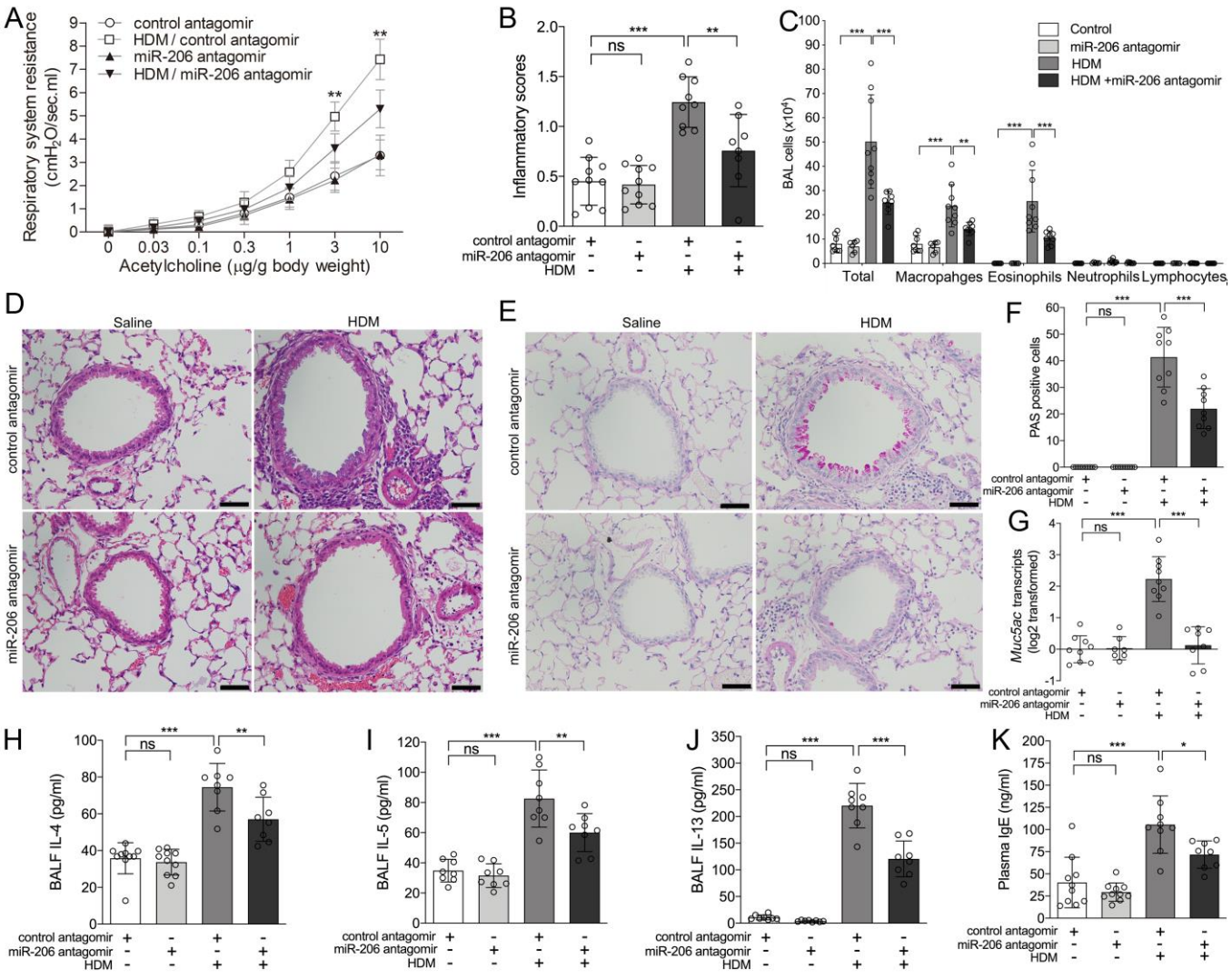
A
control antagomir
HDM / control antagomir
miR-206 antagomir
HDM / miR-206 antagomir
Respiratory system resistance (cmH2O/sec.ml)
Acetylcholine (μg/g body weight)
B
Inflammatory scores
ns
control antagomir
miR-206 antagomir
HDM
C
Control
miR-206 antagomir
HDM
HDM +miR-206 antagomir
BAL cells (x10⁴)
Total
Macropahges
Eosinophils
Neutrophils
Lymphocytes
D
Saline
HDM
control antagomir
miR-206 antagomir
E
Saline
HDM
control antagomir
miR-206 antagomir
F
PAS positive cells
G
Muc5ac transcripts (log2 transformed)
H
BALF IL-4 (pg/ml)
I
BALF IL-5 (pg/ml)
J
BALF IL-13 (pg/ml)
K
Plasma IgE (ng/ml)

Figure 6. Airway miR-206 antagonism suppresses HDM-induced AHR, airway inflammation, mucus overproduction and the type 2 response in mice. (A) Respiratory resistance in response to different concentrations of intravenous acetylcholine at 24 h after the last HDM or saline challenge in mice intranasally administered with control or miR-206 antagomir. (B) Inflammatory scores of lung sections from mice intranasally administered with control or miR-206 antagomir and challenged with HDM or saline were calculated as described in the Methods. (C) Counts of macrophages, eosinophils, lymphocytes and neutrophils in BALF. (D) H&E staining of representative lung sections. (E) PAS staining for mucus in representative lung sections. (F) The number of PAS-positive cells was counted in four random fields for each lung section at ×200 magnification. (G) *Muc5ac* transcript levels in mice lung were determined by quantitative PCR. The transcript levels are relative to the mean value of the control group and log2 transformed. (H-J) The protein levels of IL-4 (*H*), IL-5 (*I*), and IL-13 (*J*) in BALF were determined using ELISAs. (K) Plasma IgE levels in peripheral blood were determined using ELISAs. n = 6-10 mice per group combined from 2 independent experiments. The data are mean ± SD. **P* < 0.05; ***P* < 0.01; ****P* < 0.001 (one-way ANOVA with Bonferroni's post hoc test). Scale bar = 50μm.

Figure 7

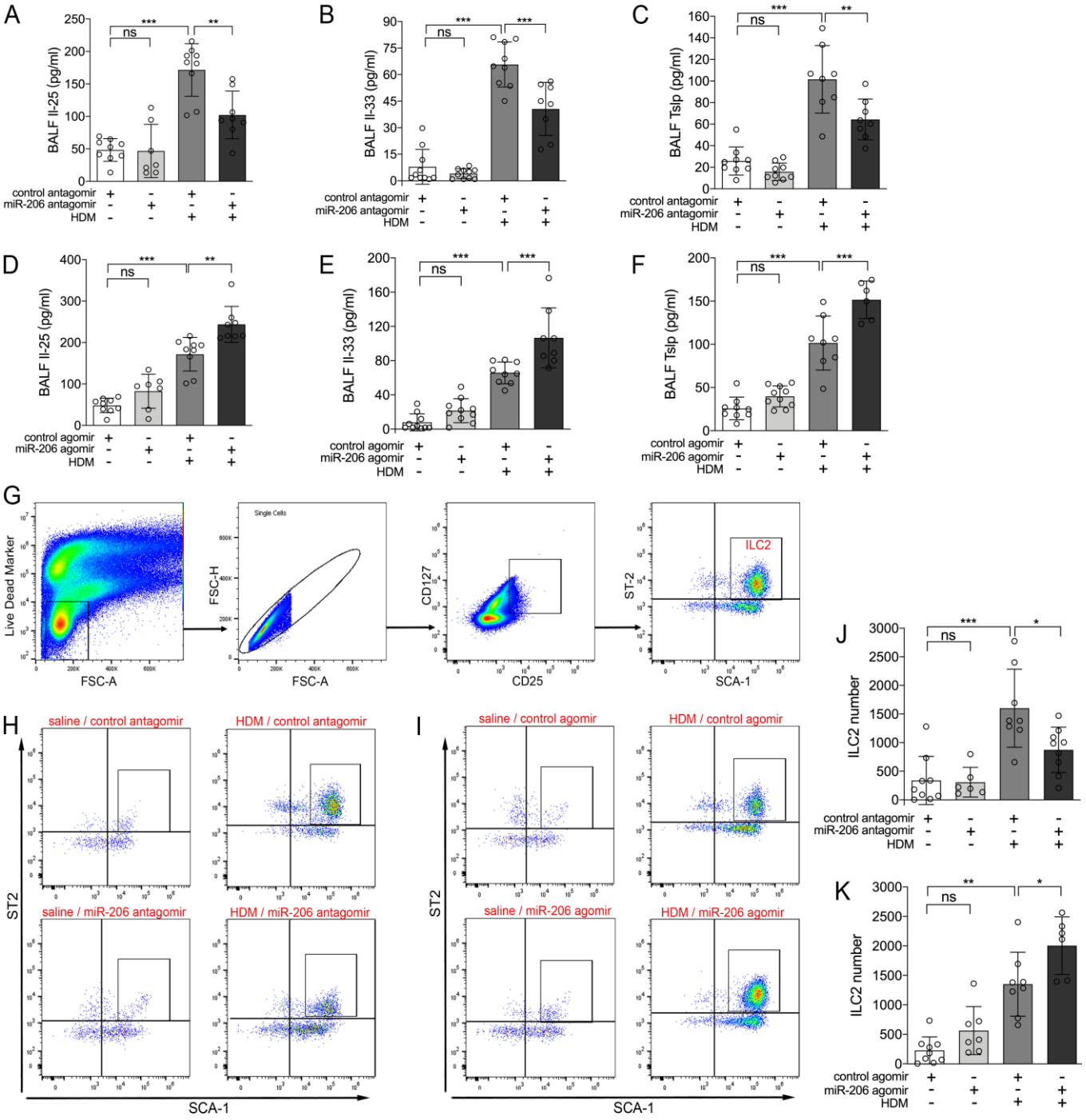
A
BALF Il-25 (pg/ml)
ns
***
**
control antagomir
miR-206 antagomir
HDM
B
BALF Il-33 (pg/ml)
C
BALF Tslp (pg/ml)
D
BALF Il-25 (pg/ml)
control agomir
miR-206 agomir
E
BALF Il-33 (pg/ml)
F
BALF Tslp (pg/ml)
G
Live Dead Marker
FSC-A
Single Cells
FSC-H
CD127
CD25
ST-2
SCA-1
ILC2
H
saline / control antagomir
HDM / control antagomir
saline / miR-206 antagomir
HDM / miR-206 antagomir
ST2
I
saline / control agomir
HDM / control agomir
saline / miR-206 agomir
HDM / miR-206 agomir
J
ILC2 number
K

Figure 7. Perturbation of airway miR-206 expression alters HDM-induced Il-25, Il-33, Tslp expression and ILC2 expansion in mouse lung. (A-C) Il-25 (*A*), Il-33 (*B*) and Tslp (*C*) protein levels in BALF were determined using ELISAs in mice intranasally administered with control or miR-206 antagomir and challenged with HDM or saline. (D-F) Il-25 (*D*), Il-33 (*E*) and Tslp protein levels (*F*) in BALF were determined using ELISAs in mice intranasally administered control or miR-206 agomir and challenged with HDM or saline. n = 6-10 mice per group combined from 2 independent experiments. (G) Single cell suspensions of mouse lung tissue were incubated with a cocktail of biotin-conjugated antibodies for detection of lineage markers and mixed with anti-Biotin microbeads to isolate lineage-negative lung cells. ILC2s in mouse lungs were enumerated via flow cytometry analysis with lineage-negative lung cells using the following gating strategy: live, single, $CD25^{+}CD127^{+}ST2^{+}Sca\text{-}1^{+}$ cells. (H, J) Representative flow cytometric plots (*H*) and numbers of ILC2s (*J*) in the lungs of mice intranasally administered control or miR-206 antagomir and challenged with HDM or saline. (I, K) Representative flow cytometric plots (*I*) and numbers of ILC2s (*K*) in the lungs of mice intranasally administered control or miR-206 agomir and challenged with HDM or saline. n = 6 – 9 per group, combined from 2 experiments. The data are mean ± SD. $*P < 0.05$; $**P < 0.01$; $***P < 0.001$ (one-way ANOVA with Bonferroni's post hoc test).

834 **Figure 8**

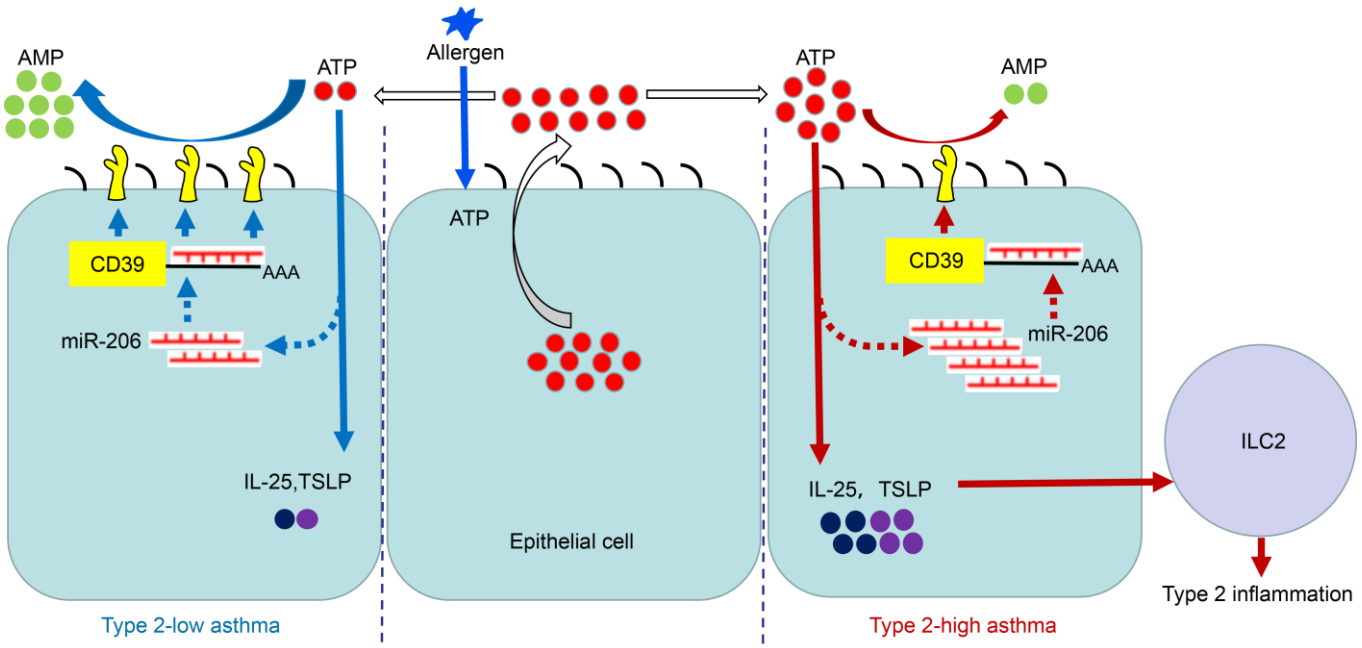

835

836

Figure 8. Scheme illustrating for the signaling pathway regulating IL-25 and TSLP expression in airway epithelial cells in type 2-low and type 2-high asthma. Allergens stimulate rapid release of ATP from epithelial cells. Extracellular ATP serves as an alarmin to induce expression of the innate cytokines IL-25 and TSLP. Meanwhile, acute accumulation of extracellular ATP decreases epithelial miR-206 expression, which upregulates CD39 expression to eliminate excessive ATP. Epithelial miR-206 is decreased in both type 2-low and type 2-high asthma. Compared with type 2-low asthma, less reduction in epithelial miR-206 results in higher miR-206 level, lower CD39 expression and impaired capacity to eliminate extracellular ATP in type 2-high asthma. Consequently, more extracellular ATP accumulates which leads to higher expression of IL-25 and TSLP and more prominent type 2 inflammation in type 2-high asthma.

Table 1. **Subjects Characteristics***

	Healthy control subjects	Type 2-low asthma patients	Type 2-high asthma patients	*p* value, type 2 low vs. high
Sample size, n	26	20	37	—
Age, yr	35.0 (28.8-42.3)	40.0 (32.3-49.5)	42.0 (31.5-50.0)	0.90
Sex, M:F (%F)	9:17 (65.3)	6:14 (70.0)	15:22 (59.5)	0.57
Body mass index	22.7 (20.6-23.8)	23.5 (21.4-25.3)	22.1 (20.6-24.0)	0.15
FEV_1, % predicted	99.0 (96.0-105.7)	82.4 (68.8-90.2)	81.6 (71.4-88.2)	0.82
Methacholine PD_{20}, mg	2.5 (2.5-2.5)	0.16 (0.04-0.25)	0.01 (0.01-0.05)	0.0009
Sputum eosinophil, %	0.3 (0-1.0)	1.8 (1.0-11.3)	16.0 (8.4-22.2)	0.0004
Blood eosinophil, $\times 10^9$/L	0.06 (0.04-0.12)	0.12 (0.07-0.23)	0.33 (0.19-0.57)	0.0003
FeNO, ppb	14.0 (11.0-17.0)	32.8 (20.3-43.7)	94.7(65.0-134.6)	< 0.0001
Serum IgE, IU/ml	27.3 (16.9-41.3)	95.0 (11.9-187.0)	150.1(72.1-335.5)	0.03
Atopic, n (%)	3 (11.5)	18 (90.0)	37 (100.0)	0.12

* Data are median (interquartile range) unless otherwise specified. *p* values comparing type 2-low with type 2-high asthma were calculated by Fisher's exact test, or Mann-Whitney U test, as appropriate. Definition of abbreviation: PD_{20} = provocative dosage required to cause a 20% decline in FEV_1. The minimal and maximal provocative dosages were 0.01 and 2.505 mg, respectively.